Chapter - 5

Apremilast loaded lyotropic liquid crystalline nanoparticles

5. Introduction

LCNPs formulations have become popular in topical drug delivery. The LCNPs formulation exhibits properties of adhesiveness, biocompatibility, biodegradability, thermodynamic stability. LCNPs can encapsulate drugs with hydrophilic and hydrophobic nature, and they can accommodate a high amount of the drug molecule in its complex structure. The LCNPs formulation exhibits high surface area, and the structure of the formulation resembles intercellular lipids of the skin. The similarity of the LCNPs with skin lipids augments the interaction and permeation of the nanoparticle. The increased permeation enhances the efficacy of the formulation. The nanosize of the formulation forms a thin layer over the skin and imparts the occlusive nature. The occlusive film formed over the skin reduces the TEWL leading to the skin's hydration and increase the gaps between corneocytes. The interaction between the skin lipid and the nanoparticle lipid increases skin retention. The complex structure of LCNPs favors the controlled release of the drug from the formulation. The present work aimed to develop the Apremilast loaded LCNPs by quality by design approach and evaluate skin retention and dermatokinetic profile on topical application. The main objective of the work was to prepare the LCNPs formulation with a size less than 200 nm and increase the permeation and skin retention of the formulation to enhance the efficacy. The LCNPs were prepared by emulsification followed by high shear homogenization, which favors easy scale-up of the formulation [1–3].

5.1. Materials

HPLC grade methanol, acetonitrile, orthophosphoric acid, methylparaben, propylparaben, and potassium dihydrogen phosphate were procured from Merck, Mumbai, India. Glyceryl monooleate (GMO) was received as a gift sample from Mohini Organics Pvt. Ltd., India. PEG 200 was obtained from CDH fine chemicals (New Delhi, India). Antibiotic-antimycotic

solution and Dulbecco's modified Eagle's medium were obtained from Thermofisher Scientific (India). Fetal bovine serum was purchased from Himedia (Mumbai, India). Carbopol® 974 P NF was received as a gift sample from Lubrizol (Belgium). Lutrol® F 127 (Poloxamer 407) and were received as gift samples from BASF (India). Cellophane tape was purchased from Scotch 3 M, USA. All other solvents, reagents, and chemicals used were of analytical grade.

5.2. Methods

5.2.1. Drug excipient compatibility study

The formulation excipients glyceryl monooleate and poloxamer 407 were evaluated for compatibility with percent assay and visual inspection. Individual excipient and drug were mixed at the ratio of 1:1, and 100 µL milli-Q water was added and stored at 30 ºC for 3 months.

5.2.2. Quality by design approach

The identification of quality target product profile and critical quality attributes, risk assessment, and optimization design selection are discussed in section 3.2.3.

5.2.3. Preparation of Apremilast LCNPs

LCNPs were prepared by emulsification technique using a high shear homogenizer. In brief, the batch quantity of GMO, Labrafil M2125, Poloxamer 407, and drug were weighed in a glass vial. The batch quantity of preservatives was added to the above mixture, and 500 µL of acetone was added to the vial to dissolve the drug and preservatives to obtain a homogeneous dispersion. The mixture was subjected to melt the lipid and evaporate the acetone at 70 ± 2 ºC. Further, 80% batch quantity of water was heated at 70 ± 2 ºC and added to the above mixture under high shear homogenization for size reduction. After size reduction, the mixture was cooled to room temperature under continuous stirring. The prepared dispersion was made up to the batch volume. The LCNPs dispersion was subjected to centrifugation at 5000 rpm for 5 min at 4°C. The supernatant dispersion was transferred to an ultracentrifuge tube (Amicon

Ultra-0.5 molecular weight cut-off 100 KDa) and centrifuged at 5,000 rpm for 30 min. The concentrated Apremilast loaded LCNPs dispersion was diluted with milli-Q up to batch volume.

5.2.4. Scale-up studies of the optimized batch

The selected batch was scaled-up to 50 mL and 100 mL. All the formulation parameters were increased proportionally, whereas all process parameters were kept constant.

5.2.5. Characterization of lipid nanocarriers

Attenuated total reflection-Fourier transform infrared spectroscopy (ATR-FTIR), Particle size, zeta, morphology, in-vitro drug release studies of Apremilast loaded LCNPs dispersion, Cytotoxicity study, Cell uptake study using Coumarin-6, and Quantitative real-time polymerase chain reaction (RT-PCR) analysis for expression of TNF-α in psoriasis induced model were performed as mentioned in section 3.2.6.

5.2.5.1. Powder X-ray diffraction

The selected formulation, drug, and physical mixture were evaluated for the crystallinity using a powder X-ray diffractometer (Rigaku- Miniflex). The analysis was performed for solid samples using the copper tube as an anode. The analysis was performed over a range of 10–40º at scattering angle of (2θ) employing an accelerating voltage of 30 kV at 25 ℃.

5.2.5.2. Entrapment efficiency

The amount of Apremilast entrapped in LCNPs formulation was determined using the direct method. The selected Apremilast loaded LCNPs dispersion was subjected to centrifugation at 5000 rpm for 5 min at 4 ℃. The supernatant dispersion was transferred to an ultracentrifuge tube (Amicon Ultra-0.5 molecular weight cutoff 100 KDa) and centrifuged at 5,000 rpm for 30 min. The concentrated Apremilast loaded LCNPs dispersion was subjected to lysis and extracted using acetonitrile. The extracted dispersion was centrifuged at 8000 rpm for 10 min,

and the supernatant was analyzed after suitable dilutions. The percent entrapment efficiency was calculated using equation 5.1

$$\%\,\text{Entrapment efficiency} = \frac{\text{Total amount of drug entrapped}}{\text{Total amount of drug added}} \times 100 \quad \text{(Eq. 5.1)}$$

5.2.5.3. Polarised light microscopy

Anisotropic liquid crystalline phases (hexagonal, lamellar, and reversed hexagonal phases) are optically birefringent. The phase identification can be made using the polarized microscope. The Apremilast loaded LCNPs dispersion was placed on the glass slide and subjected to vacuum drying for one hour to concentrate the dispersion. Then, the coverslip was placed on the dispersion and observed under a polarized light microscope (Olympus: BX53M). The birefringence was observed under 20X magnification with and without cross polariser at 25 ºC [3].

5.2.6. Preparation and characterization of Apremilast loaded LCNPs gel and free drug-loaded gel

Preparation and evaluation for rheological behavior, occlusive test, ex-vivo skin permeation studies, dermal retention studies, ex-vivo dermal distribution studies, dermatokinetic estimation were performed as mentioned in section 3.2.7 and section 3.2.8.

5.2.7. In-vivo skin retention and irritation studies

The animal study was performed with prior approved protocols by the IAEC (Protocol No. IAEC/RES/24/06/Rev-1/28/28). The animals were treated with Apremilast loaded LCNPs gel, and free drug-loaded gel and skin retention studies were performed as mentioned in section 3.2.9.2.

5.2.8. Storage stability of Apremilast loaded LCNPs gel

The selected formulation was evaluated for storage stability up to three months at 4 ℃ and 25 ℃ as mentioned in section 3.2.10.

5.2.9. Statistical analysis

All the data were statistically analyzed using either ANOVA/student's t-test as deemed fit or by other statistical evaluation parameters wherever applicable. The significance was evaluated at 95% confidence interval ($p < 0.05$).

5.3. Results and discussion

5.3.1. Drug excipient compatibility study

The results showed there was an insignificant change in percent assay (less than 1%). And there was no alteration in the physical appearance of the mixture, indicating the absence of interaction between selected excipients.

5.3.2. Quality by design approach for formulation development

The identification and classification of QTPP is the prime and key action in QbD based development. The safety and efficacy of the final product can be preferably achieved by quality parameters related to QTPP. The QTPP parameters with respect to Apremilast loaded LCNPs are listed in **Table 5.1**. CQAs identification and selection from QTPP is the secondary step of QbD design. CQAs have a prominent role in the quality of finished dosage form. Therefore, there is a need to explore their effect on formulation and monitored during the process. The CQAs with respect to Apremilast loaded LCNPs are summarized in **Table 5.2.**

5.3.3. Critical material attributes and critical process parameters

The CMAs and CPPs affecting the Apremilast loaded LCNPs quality and performance were identified. Amount of lipid and surfactant concentration were selected as CMAs, and

homogenization time was selected as the CPP. The amount of lipid and surfactant concentration has a strong influence on entrapment efficiency and particle size.

Table 5.1. The QTPP parameters with respect to Apremilast loaded LCNPs

Quality target product profile (QTPP)		
Target product profile	**Target**	**Justification**
Dosage form	LCNPs loaded hydrogel	For improved permeation and skin retention with ease of application.
Route of administration	Topical	Endorses local action with reduced systemic absorption.
Dose strength	0.05% w/w	The dose within the minimum effective concentration range
Appearance	White smooth textured gel	Soft gel free from grittiness, odour, or colour with patient acceptability.
Particle size	< 200 nm	The smaller particle size increases the occlusive nature. In addition, the small size of the formulation enhances the permeation through the stratum corneum.
Entrapment Efficiency	Maximum	Higher entrapment helps in increasing the efficacy with minimum lipid quantity (enhanced drug loading).
Drug release	Sustained release	It favors the slow release of the drug within the skin and exhibits enduring effects.

Table 5.2. Critical quality attributes of Apremilast loaded LCNPs

Critical Quality attributes	**Justification**
Entrapment efficiency	The higher the entrapment, the higher the skin permeation and skin retention.
Particle size	The smaller the particle size, the higher the occlusive effect and improved permeation.
Particle size distribution	It favors the uniform drug release, and high particle size distribution leads to irregular drug loading and fluctuation in drug release.
Drug release	The prolonged drug release favors in reducing dosing frequency with a longer duration in skin layers.
Skin retention	The higher skin retention indicates reduced systemic side effects and localized action.

Homogenization exhibits a direct impact on particle size. Additionally, the temperature, stirring time, and stirring speed influence the process and show an effect on the product quality. The material attributes, process parameters, and other independent variables affecting the finished product quality of Apremilast loaded LCNPs were identified using Ishikawa fish-bone diagram as illustrated in **Figure 5.1.**

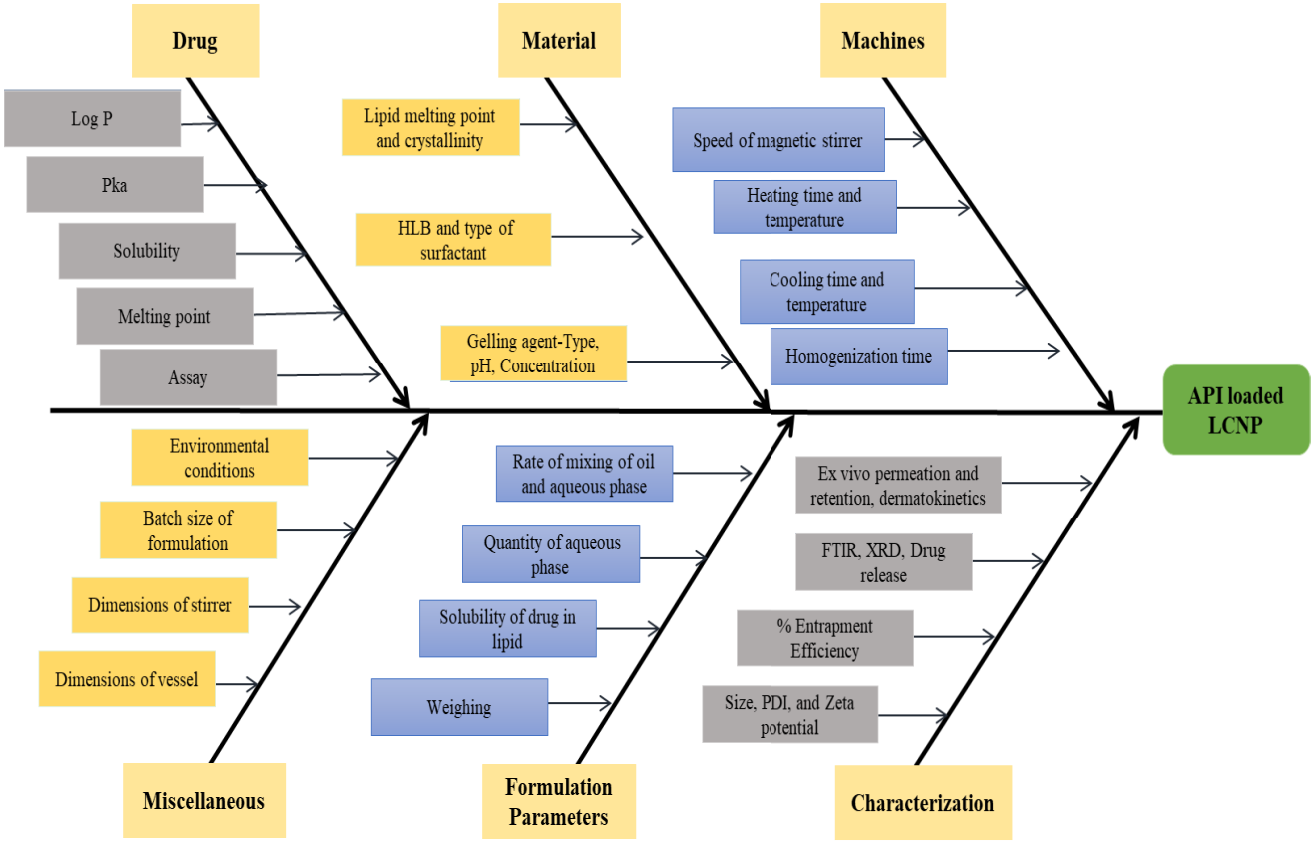

Figure 5.1. Ishikawa diagram showing the potential CMAs and CPPs that affect the CQAs of Apremilast loaded LCNPs formulation**.**

5.3.4. Risk Assessment and screening of variables

The risk assessment was performed for various factors like the amount of lipid, amount of surfactant, stirring speed, stirring time, temperature, homogenization time, homogenization speed, solvent for dissolving drug, lipid and surfactant to determine the effect on entrapment efficiency and particle size. The Risk estimation matrix analysis was performed by qualitatively

evaluating and marking the potential risk of each factor by initial trials. The amount of lipid, amount of surfactant and homogenization time were found to exhibit a high impact on the entrapment efficiency and particle size. The risk priority number score was allotted based on the available literature, initial trials and factors were selected for screening. The risk assessment matrix to determine the critical material attributes and process parameters is represented in **Table 5.3.**

Table 5.3. Risk estimation matrix to determine the critical material attributes and process parameters.

Critical Quality attributes	**Critical material attributes and process parameters**					
	Amount of lipid	**Amount of surfactant**	**Homogenization time**	**Temperature**	**Stirring speed**	**Stirring time**
Entrapment efficiency	High	High	High	Low	Low	Medium
Particle size	High	High	High	Medium	Medium	Low
Polydispersity index	Medium	High	High	Medium	Medium	Low
Drug release	High	High	Medium	Low	Low	Medium

5.3.5. Design of experiment for optimization

The Box Behnken optimization design was employed to optimize Apremilast loaded LCNPs dispersion. Box Behnken can be employed for interaction between input variables with the least number of experiments and allows the optimization, evaluation and estimation of the formulation. The amount of lipid, amount of surfactant (material attributes) and homogenization time (process attributes) were selected for design as the independent variables at three levels. All other materials and process parameters were kept constant, including drug concentration and batch size. The entrapment efficiency and particle size were selected as the response (dependent) variables. Using Design-Expert® 8.06 (Stat Ease, Inc., Minneapolis, USA), 17 experiments were generated with three centre points (three factors and three levels). The 17 runs generated were executed arbitrarily to counteract the effect of impeding or

extraneous factors. The model efficiency and the significance of selected input factors were verified by ANOVA. The values of response variables obtained for the experimental runs of Apremilast loaded LCNPs DoE batches are presented in **Table 5.4.**

Table 5.4. The values of independent variables and response variables of Box Behnken trials.

S.No.	Lipid (mg)	Surfactant (%)	Homogenization time (min)	Particle size (nm)	% Entrapment	PDI
1	100	0.75	10.00	155.30 ± 2.19	73.91 ± 2.44	0.426
2	50	0.50	10.00	134.90 ± 6.88	17.63 ± 5.31	0.284
3	100	0.50	15.00	227.80 ± 12.65	60.59 ± 4.48	0.245
4	100	0.75	10.00	173.80 ± 4.45	83.42 ± 6.14	0.330
5	100	0.50	5.00	232.50 ± 9.13	62.83 ± 5.02	0.250
6	100	0.75	10.00	168.30 ± 7.73	70.08 ± 1.57	0.281
7	150	0.75	15.00	183.90 ± 5.65	78.52 ± 1.03	0.267
8	150	0.50	10.00	253.20 ± 8.34	62.07 ± 1.93	0.259
9	100	0.75	10.00	186.80 ± 6.13	76.75 ± 9.80	0.400
10	100	0.75	10.00	156.40 ± 8.17	74.52 ± 4.39	0.344
11	100	1.00	5.00	189.90 ± 11.60	67.19 ± 3.64	0.635
12	150	1.00	10.00	191.30 ± 10.43	83.03 ± 4.61	0.462
13	50	0.75	15.00	200.40 ± 11.01	46.83 ± 7.16	0.288
14	50	0.75	5.00	140.76 ± 12.12	55.29 ± 3.11	0.428
15	150	0.75	5.00	240.90 ± 6.91	83.43 ± 6.83	0.281
16	50	1.00	10.00	105.20 ± 9.71	53.25 ± 5.97	0.932
17	100	1.00	15.00	157.00 ± 7.70	69.13 ± 4.93	0.468

*The data mentioned is the average of experiments performed in replicates (n=3). PDI was not considered as the response variable. (Low lipid – 50 mg; Medium lipid – 100 mg; High lipid – 150 mg; Low surfactant – 0.50 %; Medium surfactant – 0.75 %; High surfactant – 1.00 %; Low homogenization time – 5.00 min; Medium homogenization time – 10.00 min; High homogenization time – 15.00 %)

5.3.5.1. Effect of independent variables on particle size

The average particle size of Apremilast-loaded LCNPs of 17 experiments was in the range of 105.2 to 253.2 nm. The response surface quadratic model F-value was 6.46, which indicates that the model was significant. The ANOVA for the responses is represented in **Table 5.5**. The contour plot graph and 3D plot graph of the particle size are represented in **Figure 5.2 A and**

Figure 5.2 B. The lack of fit of the model was insignificant compared to the pure error with an F-value of 4.07. The regression equation of particle size in terms of coded values of chosen independent factors is represented in equation 5.2.

$$\text{Size} = 127.995 + 2.6607A - 141.78b - 6.588C - 0.644AB - 0.11664AC - 5.64BC - 0.00146A^2 + 106.72B^2 + 1.0804C^2 \quad \text{(Eq. 5.2)}$$

The regression equation's (+) positive symbol represents the positive quantitative effect on response value with the respective input variable. The regression equation's (-) negative symbol represents a decrease in response value with the respective input variable. The observed R-square (0.89258) and the adjusted R-square (0.754473) values exhibited a close agreement with less than 0.2 variations. The lack of fit indicates the competence of the model fitting to the experimental results and affords dissimilarity in the best fit model's data. The insignificant lack of fit in experimental results indicated the best fit for the model. The regression equation suggested an increase in particle size with an enhancement in the amount of lipid. A reduction in particle size was observed with an increase in surfactant concentration and homogenization time. The increase in the surfactant concentration reduces the interfacial tension between the lipid and water phases due to stabilizing particles.

Similarly, the homogenization time has an impact on size reduction. An increase in homogenization time reduces the particle size, breaking the large particles into smaller particles. The increase in the amount of surfactant and homogenization time has reduced the particle size of LCNPs. The S/N ratio of the model was found to be 9.407, indicating the adequacy of the model.

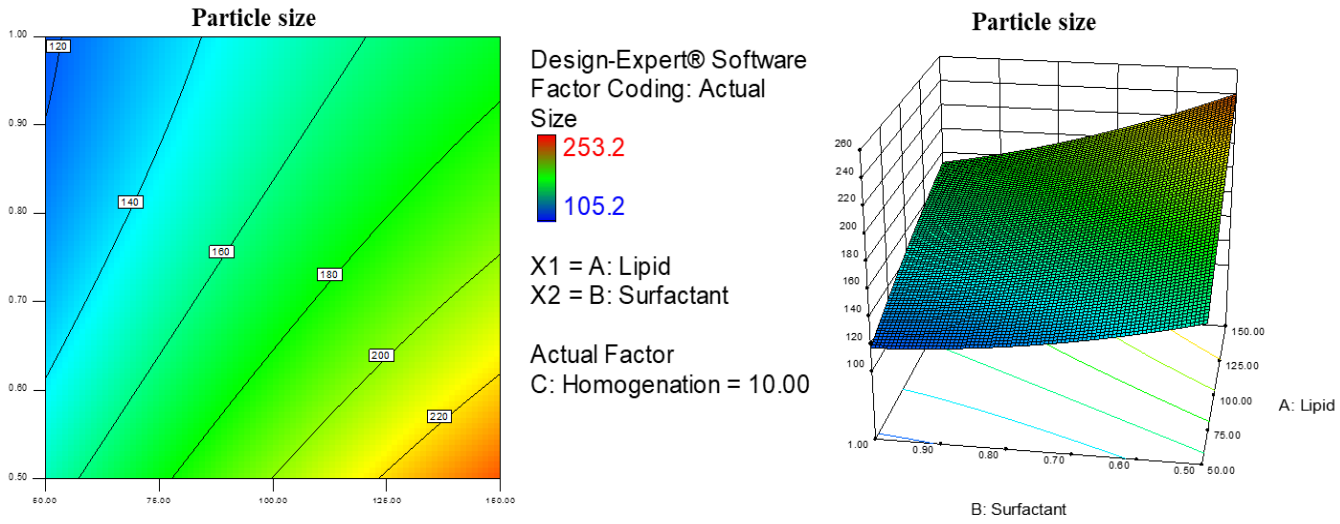

Figure 5.2 A. The contour plot graph indicating the effect of independent variables on the particle size of Apremilast loaded LCNPs. **Figure 5.2 B.** The 3D graph indicating the effect of independent variables on the particle size of Apremilast loaded LCNPs.

5.3.5.2. Effect of independent variables on entrapment efficiency

The average entrapment efficiency of Apremilast-loaded LCNPs of 17 experiments was in the range of 17.62 to 83.43%. The response surface quadratic model F-value was 8.11, which indicates that the model was significant. The contour plot graph and 3D plot graph of the entrapment efficiency were represented in **Figure 5.3 A** and **Figure 5.3 B**. The lack of fit of the model was found to be insignificant compared to the pure error with an F-value of 3.93. The regression equation of particle size in terms of coded values of chosen independent factors is represented in equation 5.3.

$$\text{Entrapment efficiency} = -134.154 + 1.346072A + 329.5501B - 1.81478C - 0.29308AB + 0.003548AC + 0.837536BC - 0.00413A^2 - 182.5836B^2 + 0.034501C^2 \quad \text{(Eq. 5.2)}$$

The regression equation's (+) positive symbol represents the positive quantitative effect on response value with the respective input variable. The regression equation's (-) negative symbol represents a decrease in response value with the respective input variable. The observed R-square (0.912469), and the adjusted R-square (0.799929) values were found to be in close

agreement with each other with less than 0.2 variations. The best fit for the model was indicated by the insignificant lack of fit in experimental results.

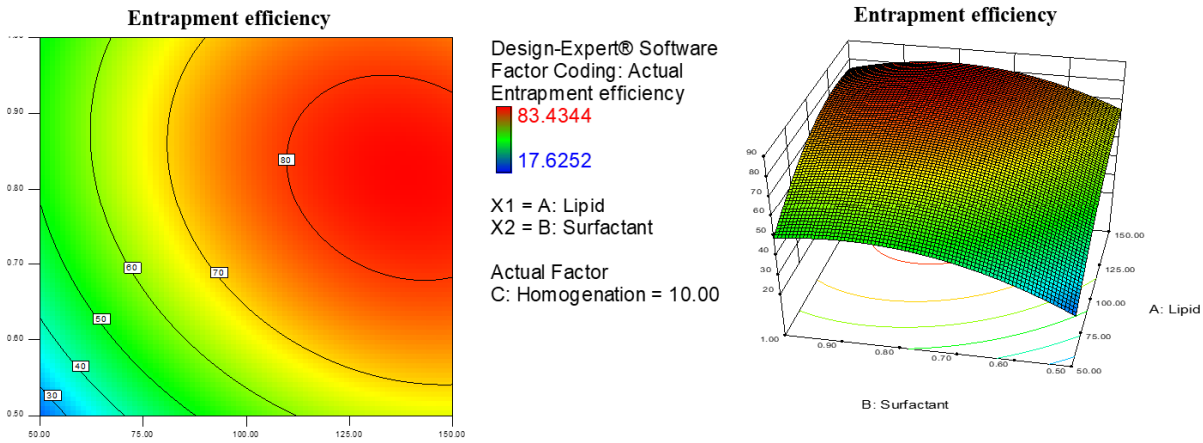

Figure 5.3 A. The contour plot graph indicating the effect of independent variables on the entrapment efficiency of Apremilast loaded LCNPs. **Figure 5.3 B.** The 3D graph showing the effect of independent variables on the entrapment efficiency of Apremilast loaded LCNPs.

Table 5.5. ANOVA for response Particle Size and Entrapment efficiency.

Response	**Particle Size**		**Entrapment efficiency**	
Source	F-value	p-value	F-value	p-value
Model (significant)	6.462895	0.0112	8.107952	0.0058
A- Amount of lipid	26.23042	0.0014	41.09868	0.0004
B-Surfactant concentration	13.2864	0.0082	11.03943	0.0127
C-Homogenization time	0.386405	0.5539	0.427376	0.5342
AB	0.655604	0.4448	0.98193	0.3547
AC	8.6025	0.0219	0.057566	0.8173
BC	0.502838	0.5012	0.080189	0.7852
A^2	0.141101	0.7183	8.221117	0.0241
B^2	0.473781	0.5134	10.02866	0.0158
C^2	7.76918	0.0270	0.028893	0.8698

The regression equation suggests an increase in entrapment efficiency with enhancement in the amount of lipid and amount of surfactant. The increase in the amount of lipid favors increased drug solubility due to the interaction between the lipid phase, further increasing entrapment

efficiency. The increase in the amount of surfactant has a positive effect as it maximizes lipid utilization in nanoparticle formation. This maximum utilization of the lipid increases entrapment efficiency. The regression equation describes the increase in homogenization time and reduces the entrapment efficiency. Whereas the interaction of lipid, homogenization, and surfactant, homogenization positively affects the entrapment efficiency. The maximum lipid was utilized by the increase in homogenization time and surfactant concentration. This favors the increase in entrapment efficiency. The S/N ratio of the model was found to be 10.353, indicating the adequacy of the model.

5.3.6. Validation of the design to select optimized batch

The obtained design space was validated using the numerical desirability method. The independent variables were chosen to the optimum level to optimize the LCNPs formulation with small particle size and highest entrapment efficiency. The constraint criteria selected to attain the desired response variable are summarized in **Table 5.6**. The suggested solution with a desirability value near 1 (0.844) was selected from the obtained solutions. The desirability contour plot, with maximum entrapment efficiency and minimum particle size, is shown in **Figure 5.4**.

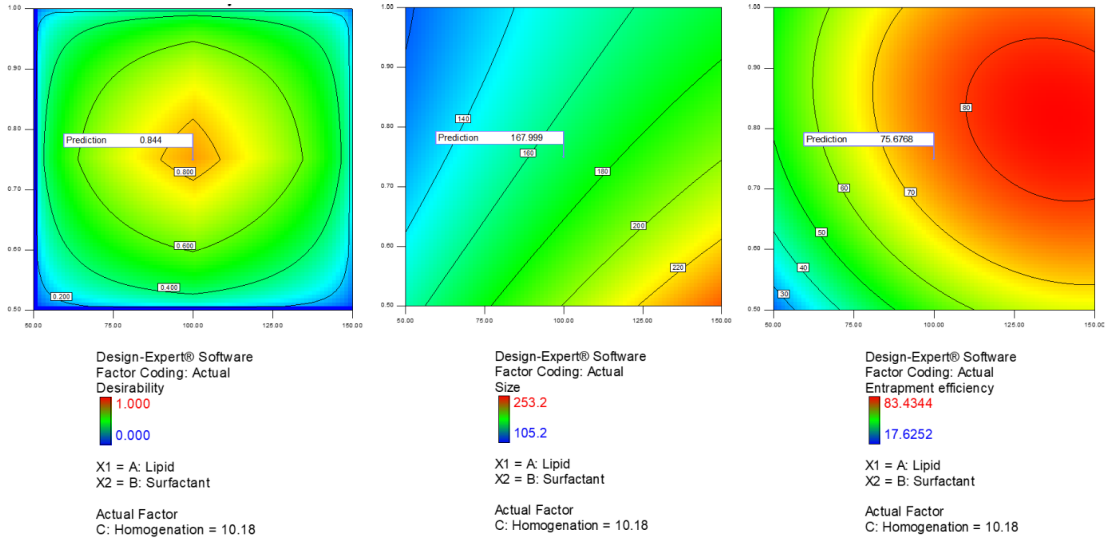

Figure 5.4. The desirability contour plot, with maximum entrapment efficiency and minimum particle size.

Table 5.6. Constraint criteria for achievement of desired response variable and deviation (%) obtained in validation batch of Apremilast loaded LCNPs dispersion.

Parameter	**Goal**	**Lower Limit**	**Upper Limit**
A: Amount of lipid (mg)	In range	50	150
B: Surfactant concentration (%)	In range	0.5	1.0
C: Homogenization time (min)	In range	5	15
Particle size (nm)	Minimize	105.20	253.20
EE (%)	Maximize	17.63	83.43
Deviation (%) calculation of Apremilast-LCNPs formulation.			
Parameter	**Predicted values**	**Actual values**	**% Deviation**
Particle size (nm)	167.99	173.25 ± 2.192	5.251
% EE	75.68	75.028 ± 0.235	0.650

The optimized formulation selected contained 100 mg lipid, 0.75 % surfactant and 10.18 min homogenization time, showing 0.844 desirability. The optimized batch was executed. The particle size and entrapment efficiency of the formulation were found to be 173.25 ± 2.192 nm (PDI 0.273 ± 0.008) and 75.028 ± 0.235 %, respectively. The obtained results were found to be near to the predicted values, indicating the desirability of the design. The deviation of predicted particle size and entrapment efficiency was 5.251 nm and 0.65%, respectively.

5.3.7. Scale-up of the optimized batch

The selected formulation was further evaluated for scale-up capability. The optimized batch of 10 mL formulation was scaled up to 50 mL and 100 mL. The parameters similar to the centre point were used for the preparation of the scale-up baches. The particle size and entrapment of 10 mL, 50 mL, and 100 mL batches are listed in **Table 5.7**. There was minimal difference between the size (< 30.4 nm) and entrapment efficiency (< 0.743%), indicating scalability of the Apremilast loaded LCNPs formulation. The particle size graph is illustrated in **Figure 5.5**. The zeta potential of the LCNPs formulation was found to be –21.46 ± 1.30 mV (as shown in

Figure 5.6). The morphology of the selected formulation is illustrated in **Figure 5.7.** The particle size of the formulation was in the range of 84.98 nm to 173.50 nm.

Table 5.7. The particle size and entrapment of 10 mL, 50 mL and 100 mL batches.

Batch Size	**10 mL**	**50 mL**	**100 mL**
Particle size (nm)	187.233 ± 2.06	156.833 ± 5.840	180.067 ± 1.662
PDI	0.274 ± 0.009	0.251 ± 0.019	0.264 ± 0.033
Entrapment efficiency (%)	75.144 ± 0.601	74.401 ± 0.849	74.660 ± 0.467

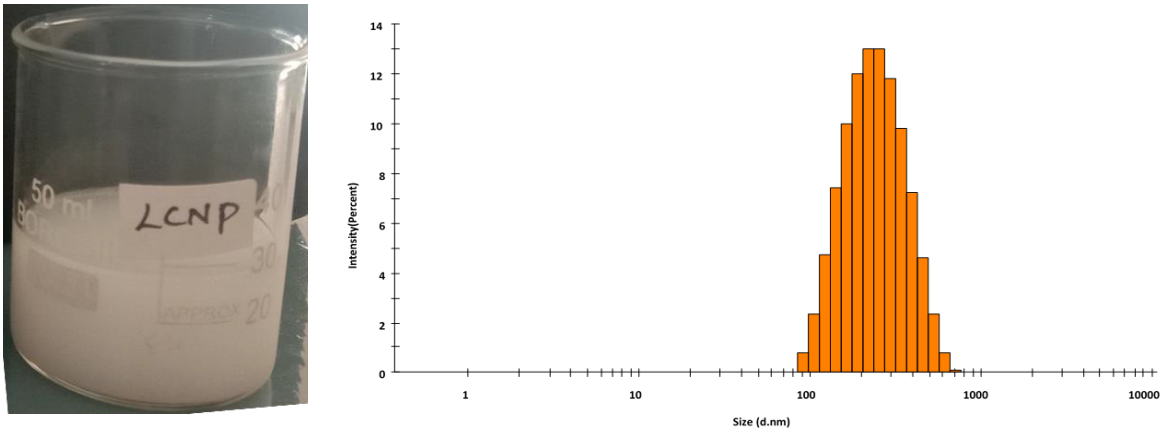

Figure 5.5. Apremilast loaded LCNPs dispersion and particle size statistics graph.

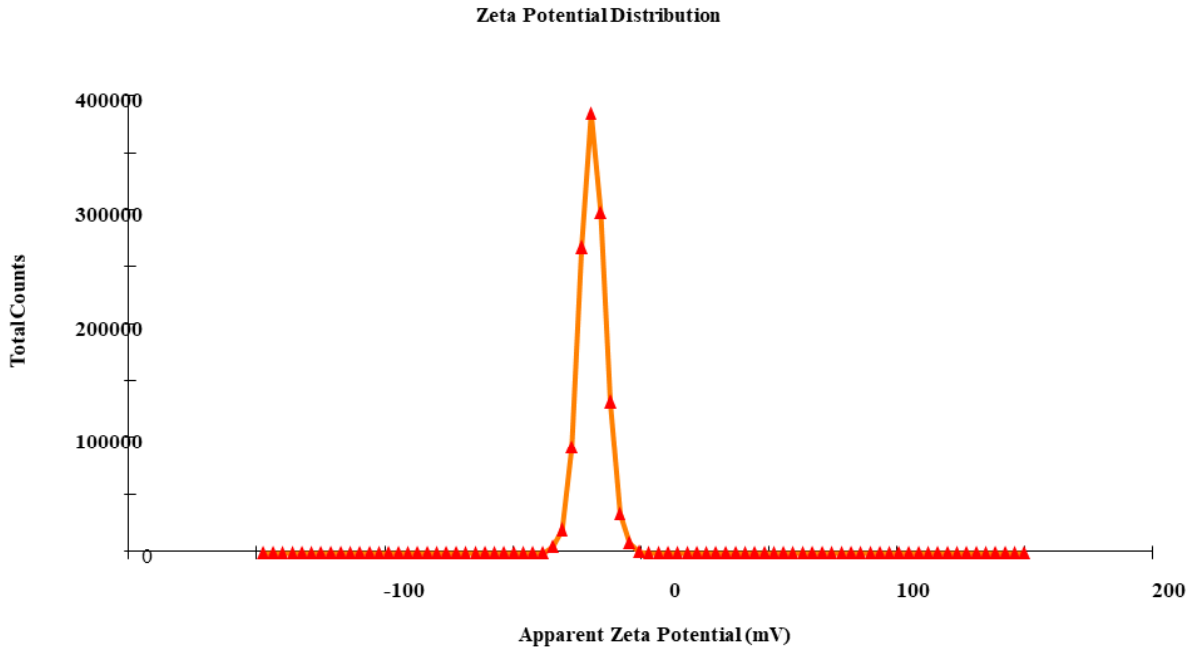

Figure 5.6. Apremilast loaded LCNPs dispersion zeta potential graph.

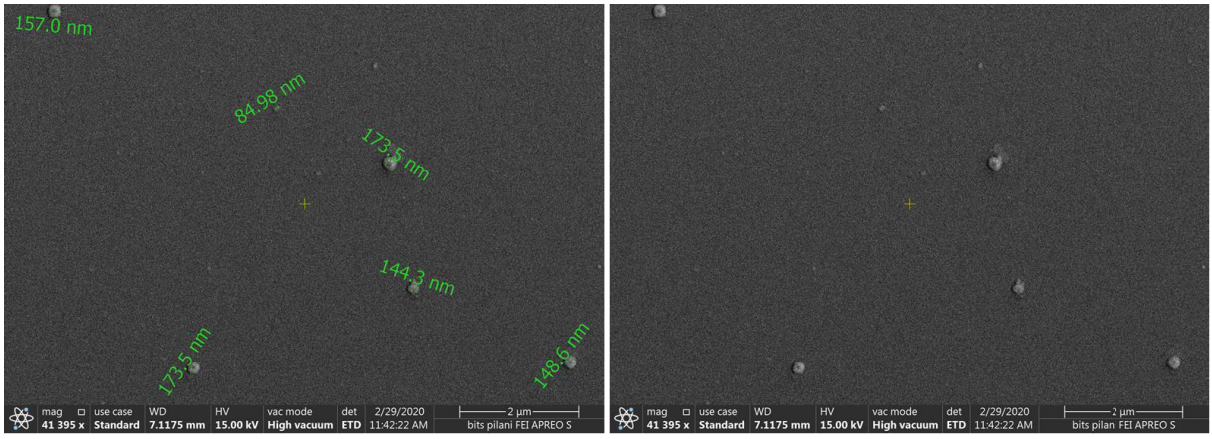

Figure 5.7. The morphology of the LCNPs formulation.

5.3.8. Characterization of Apremilast loaded LCNPs dispersion

5.3.8.1. Compatibility of selected excipients

The significant interaction between the selected excipients and the drug was evaluated by generating ATR spectra of the pure drug, physical mixture, and Apremilast loaded LCNPs dispersion. The amide group of Apremilast exhibits peaks in the range of 3100 and 3500 cm^{-1}. The peaks in the range of 1600 cm^{-1} and 1300cm^{-1} indicate the alkene (C=C) and alkane (C-C) bonds. The presence of ester (C-O) and C-OH group peaks were observed in the range of 1000 cm^{-1} and 1100 cm^{-1}. The ATR spectra of the drug, physical mixture, and LCNPs formulation are shown in **Figure 5.8**. The study demonstrates that there was no interaction between the drug and other formulation excipients, indicating excellent compatibility.

5.3.8.2. Powder X-Ray diffraction

The X-ray diffraction studies confirm the characteristic structural differences between drug and LCNPs formulation. The X-ray diffraction was recorded for Apremilast, physical mixture and LCNPs formulation. The diffractograms are represented in **Figure 5.9**. The Apremilast peaks disappeared in the LCNPs formulation, and sharp peaks were observed indicating LCNPs formulation. The liquid-like order arrangement within LCNPs layers leads to the diffusion of

four spot wide-angle patterns. This was expected due to hidden first-order reflection by beam stop, alignment of signals on the equator showing the planes lie parallel [2,4].

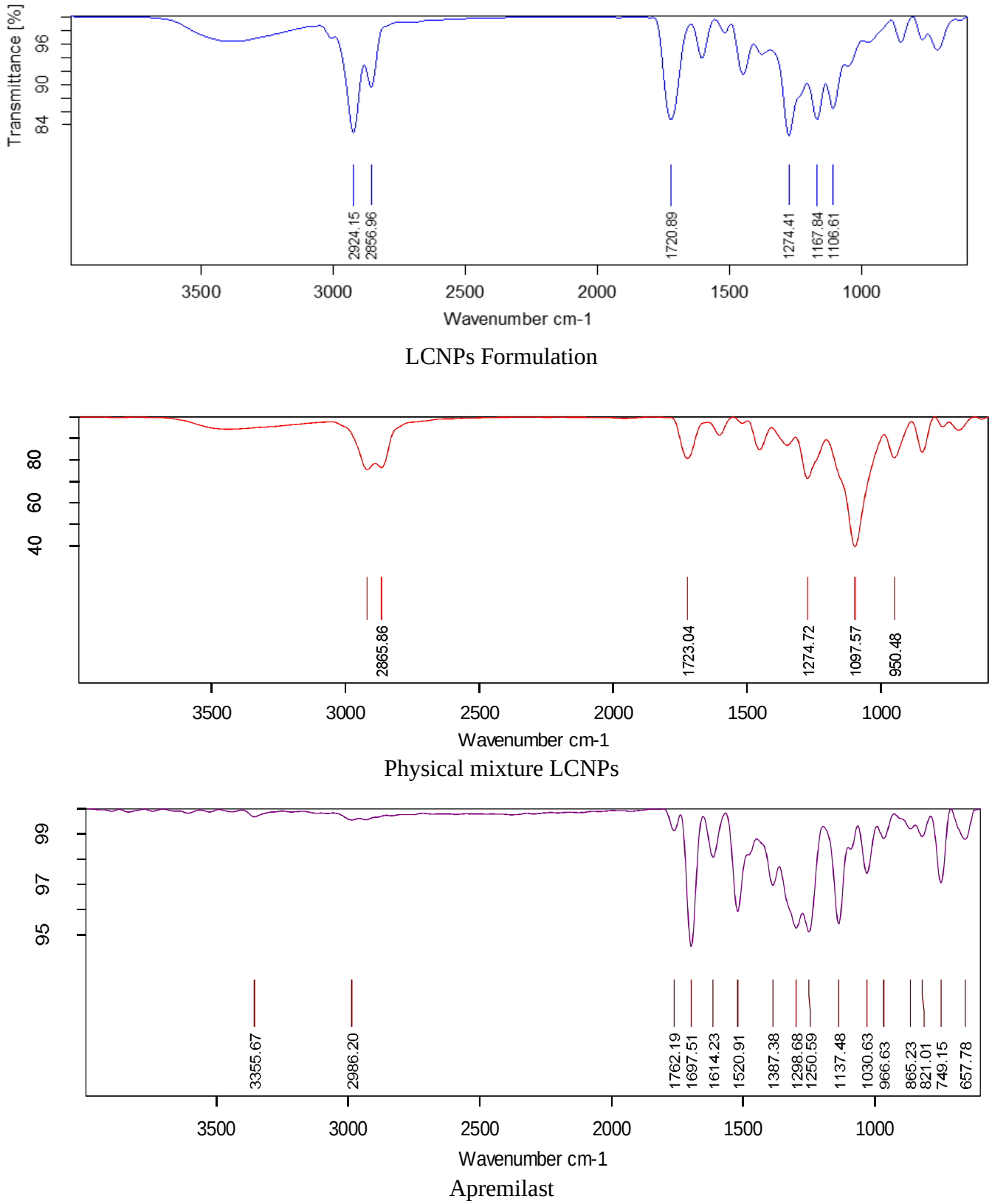

Figure 5.8. The ATR spectra of the drug, physical mixture, and LCNPs formulation

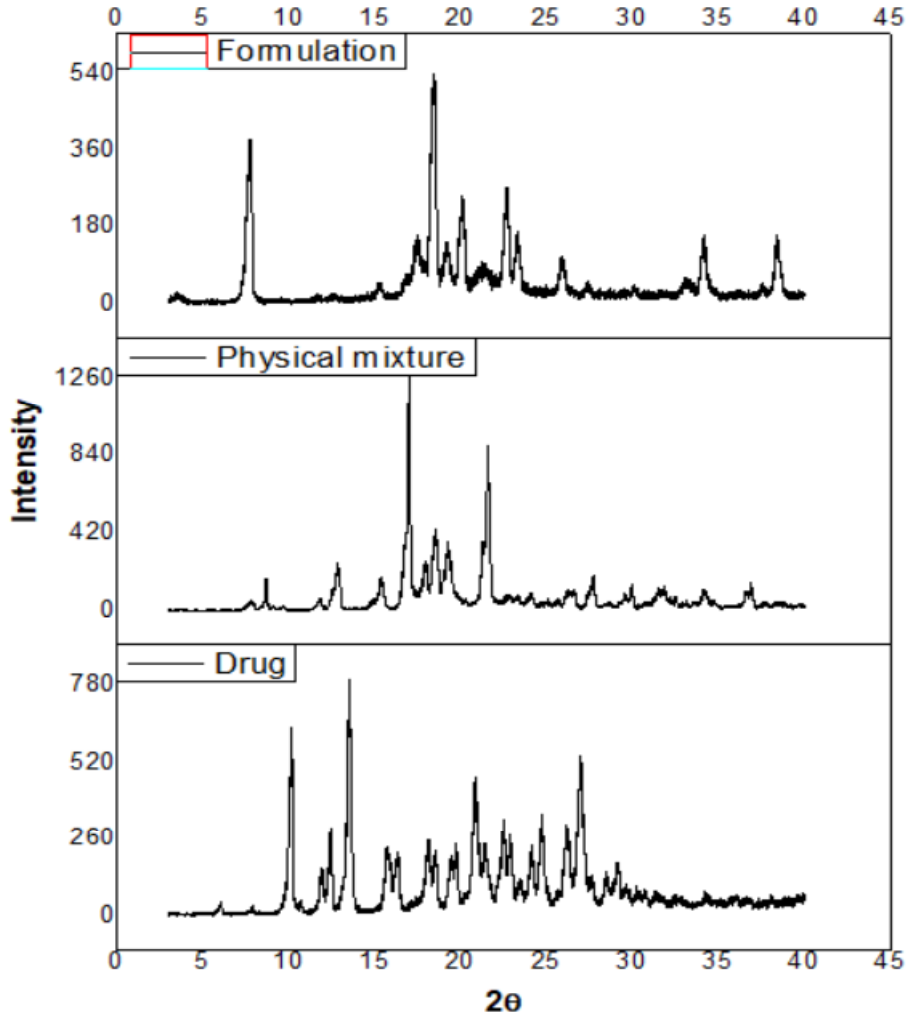

Figure 5.9. The powder X-Ray diffractogram of the Apremilast LCNPs formulation.

5.3.8.3. Polarised light microscopy

The polarised light microscopy of the selected formulation is shown in **Figure 5.10.** The results indicated that the obtained formulation exhibits birefringence, indicating that the formed LCNPs were hexagonal, lamellar, and reversed hexagonal phases. As the micellar, reversed micellar, and cubic phases show a dark background. The formed LCNPs were hexagonal columnar morphology signifying the crystalline nature of the formulation. The formulation had a liquid-like appearance and internally had crystalline nature, thus confirming that the prepared formulation had properties of both liquid and a solid crystal [3].

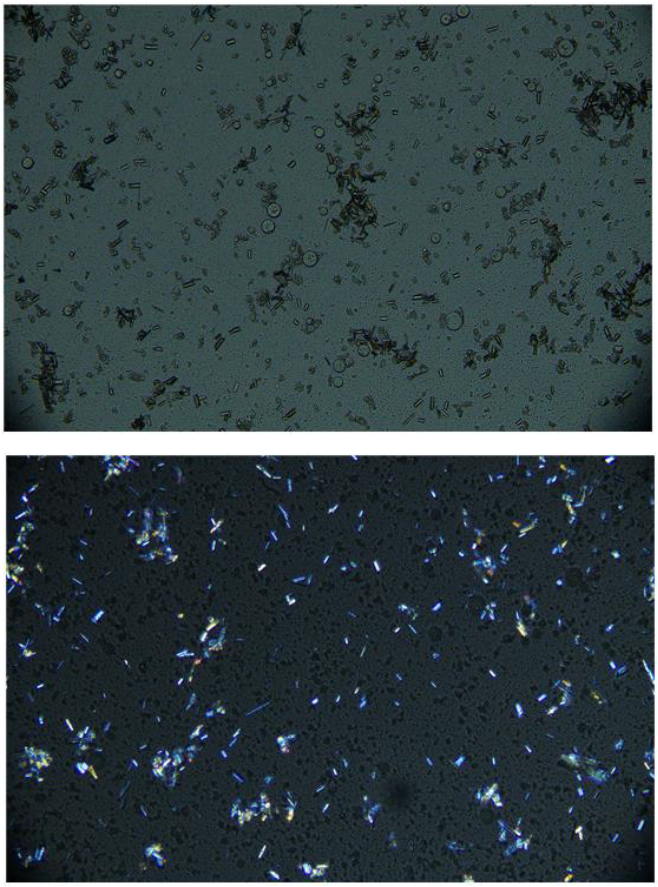

Figure 5.10. The polarized light microscopic images of the Apremilast loaded LCNPs dispersion (without and with cross polarizer)

5.3.8.4. In-vitro drug release studies

The in-vitro drug release study was performed for Apremilast loaded LCNPs dispersion (10 mL, 50 mL, and 100 mL batch size) and free drug. The free drug exhibited 100% release within 6 h, whereas the drug release from formulation was observed for 18 h. The in-vitro release profile of data is showed in **Figure 5.11**. The obtained release data were found to be the best fitted into the first-order release mechanism with regression value (R^2) 0.987 and low AIC (Akaike information criterion) value 52.793. The results of various mathematical models are showed in **Table 5.8**. The n value of the formulation was less than 0.5, indicating Fickian diffusion. Therefore, the solubility of the drug in the lipid favored the controlled release of drug from Apremilast loaded LCNPs dispersion.

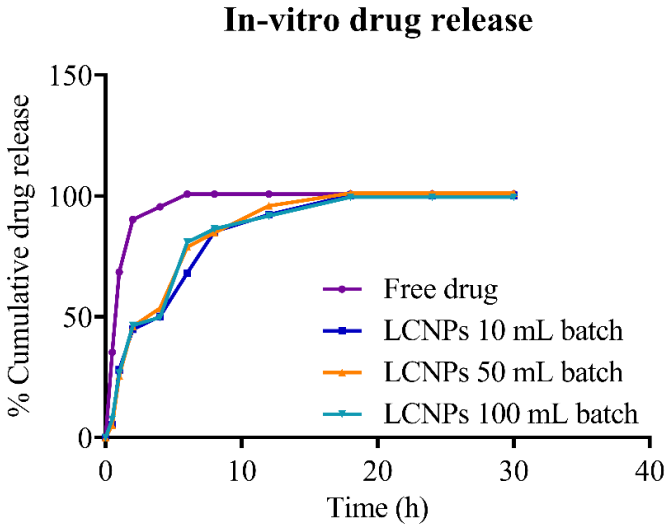

Figure 5.11. The in-vitro release profile of Apremilast loaded LCNPs dispersion.

Table 5.8. Release kinetic data of Apremilast loaded LCNPs dispersion (n=6)

Batch Size		**Zero-order**	**First-order**	**Higuchi**	**Korsmeyer-Peppas**	**Hixson-Crowell**
10 mL	**R^2**	0.902	0.986	0.976	0.978 (n=0.465)	0.984
10 mL	**AIC**	76.856	52.973	57.990	59.511	55.917
50 mL	**R^2**	0.886	0.991	0.971	0.976 (n=0.460)	0.989
50 mL	**AIC**	78.282	49.747	60.688	61.188	52.661
100 mL	**R^2**	0.878	0.987	0.965	0.969 (n=0.442)	0.985
100 mL	**AIC**	78.701	52.793	61.788	62.782	55.662

5.3.8.5. Cytotoxicity and cell uptake study

The cytotoxicity of Apremilast loaded LCNPs dispersion on HaCaT cells showed that the formulation was non-toxic. The MTT assay results are represented in **Figure 5.12.** The free Apremilast solution and Apremilast loaded LCNPs dispersion showed an IC_{50} value of 20 nM [5]. The Coumarin-6 loaded LCNPs uptake results revealed C_6/DAPI ratio of LCNPs dispersion was found to be higher compared (3.13 and 21.94) to free Coumarin-6 (in 1 h and 3 h) (***$p<0.0001$). The cell uptake intensity and cell uptake fluorescence images are showed in **Figures 5.13 A and 5.13 B.** The nano-size, the fatty acid chain lipid in LCNPs dispersion and cell membrane interaction are expected to be the reason for high uptake [6].

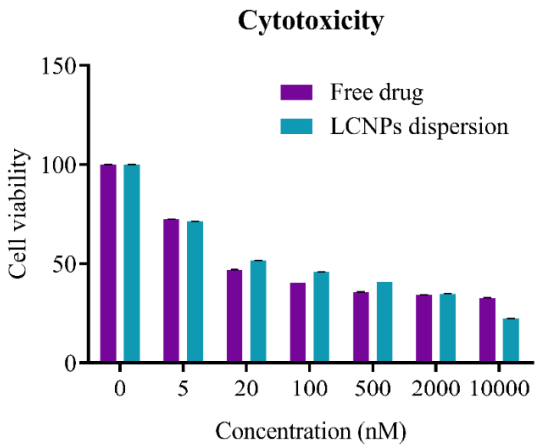

Figure 5.12. The MTT assay of Apremilast loaded LCNPs dispersion on HaCaT cell lines.

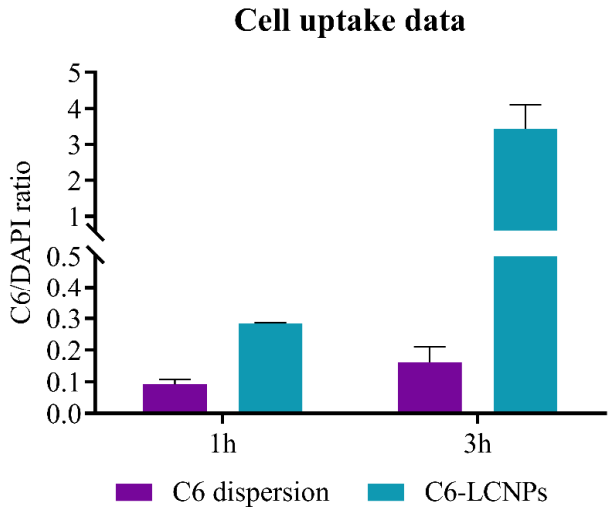

Figure 5.13 A. The cell uptake intensity of Coumarin-6 loaded LCNPs dispersion.

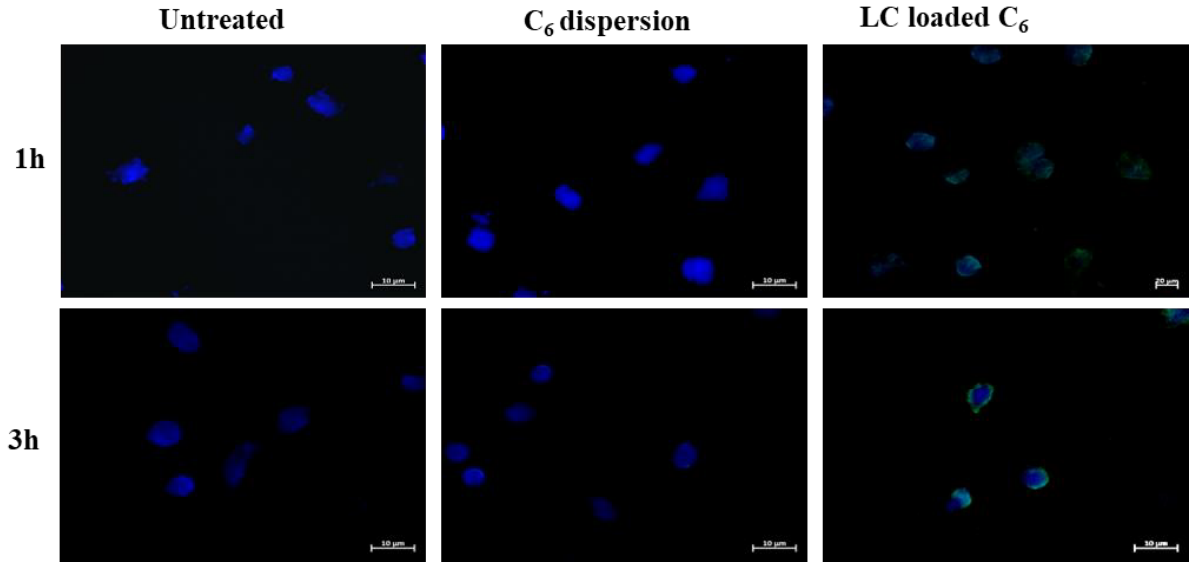

Figure 5.13 B. The cell uptake fluorescence images of Coumarin-6 loaded LCNPs dispersion.

5.3.8.6. Expression of TNF-α in psoriasis induced model

The Apremilast loaded LCNPs dispersion and free Apremilast efficacy in reduction of TNF-α was evaluated in in-vitro imiquimod-induced psoriasis. The RNA was isolated initially, and gene expression was quantified and normalized to GAPDH. The cycle threshold (Ct) values were altered to perceptible levels after treating with LCNPs and free Apremilast, as portrayed in **Figure 5.14.** There was a 3.73 fold more significant C_t value reduction with LCNPs dispersion and 1.6 fold with the free drug than the positive control (***p<0.0001; one-way ANOVA was performed). As represented in the cell uptake study, high internalization of Apremilast was observed in LCNPs dispersion. This reduces the relative mRNA level expression of TNF-α, which further reduces the inflammatory mediators [7–9].

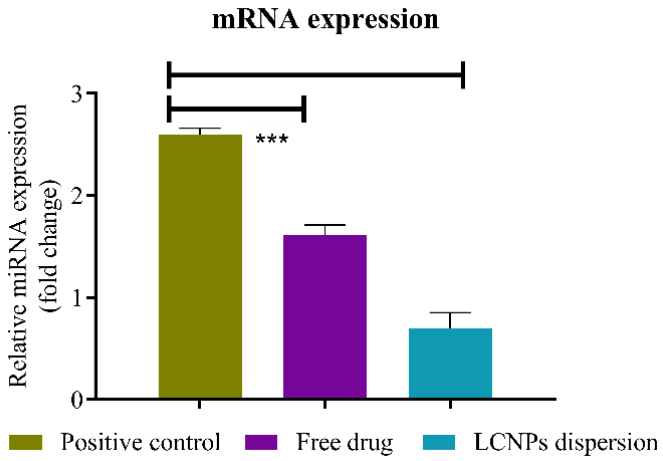

Figure 5.14. The relative reduction of TNF-α mRNA in the imiquimod induced psoriasis model (n=3) (**p<0.005).

5.3.9. Gel characterization

5.3.9.1. Rheological behavior and Occlusive Test

The Apremilast LCNPs were loaded in a 0.75% Carbopol gelling agent. The viscosity of the gel was found to be 6777 mPa.s. The gel exhibited Newtonian behaviour, as there was no remarkable change in viscosity with change in time, gel structure fully persisted [10,11]. The amplitude sweep test revealed that the gel exhibited linear viscoelastic properties and solid-like

properties at low strain. After the critical strain of 0.0124%, the gel storage modulus was reduced. The frequency sweep test demonstrated the high stability of gel with no variation in storage modulus (G'). The high crosslinking between the Carbopol increases the strength of the gel. The results depicted that the gel can withhold maximum strain with substantially greater storage modulus (G') contrasted to loss modulus (G") [12,13]. The rheological properties of Apremilast loaded LCNPs gel are illustrated in **Figure 5.15 (A-D)**.

The in-vitro occlusive study revealed that the Apremilast loaded LCNPs gel exhibited high occlusive nature (occlusive factor 51.471 ± 0.305 in 48 h) (reduce percentage water loss) in comparison to free drug-loaded gel (occlusive factor 8.302 ± 0.587 in 48 h) (**Figure 5.16)**. In addition, the high occlusive nature of LCNPs gel reduces TEWL by forming a thin film layer. This enhances the skin permeation on topical application by hydrating the skin [14].

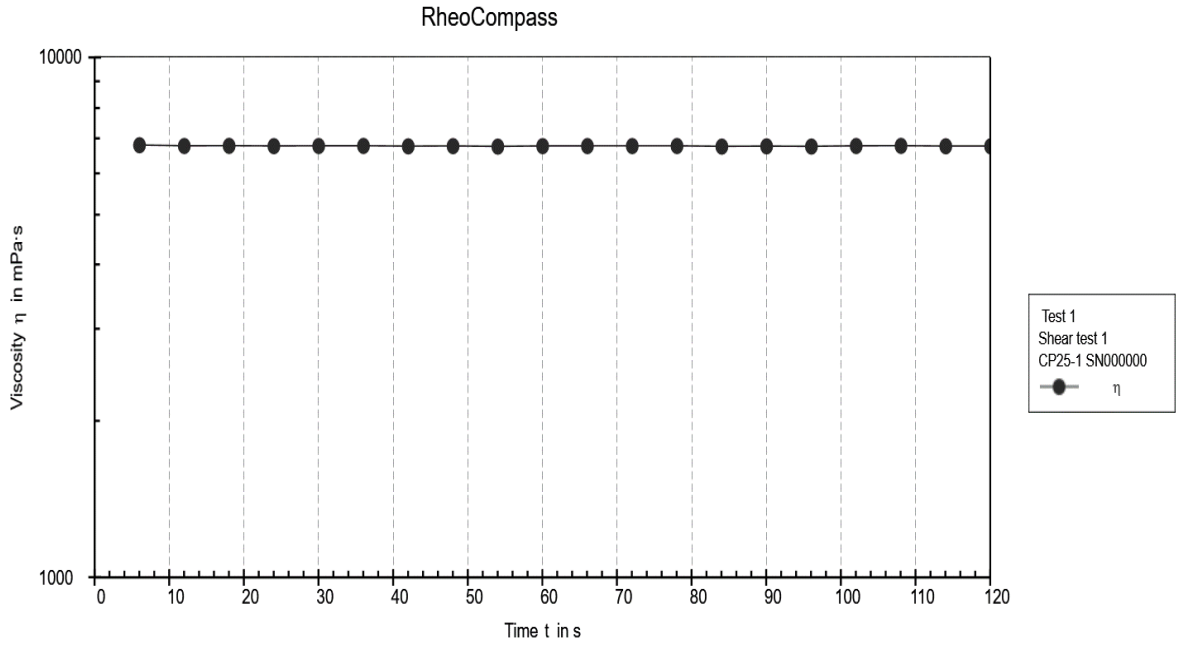

Figure 5.15 A. The viscosity of Apremilast loaded LCNPs gel

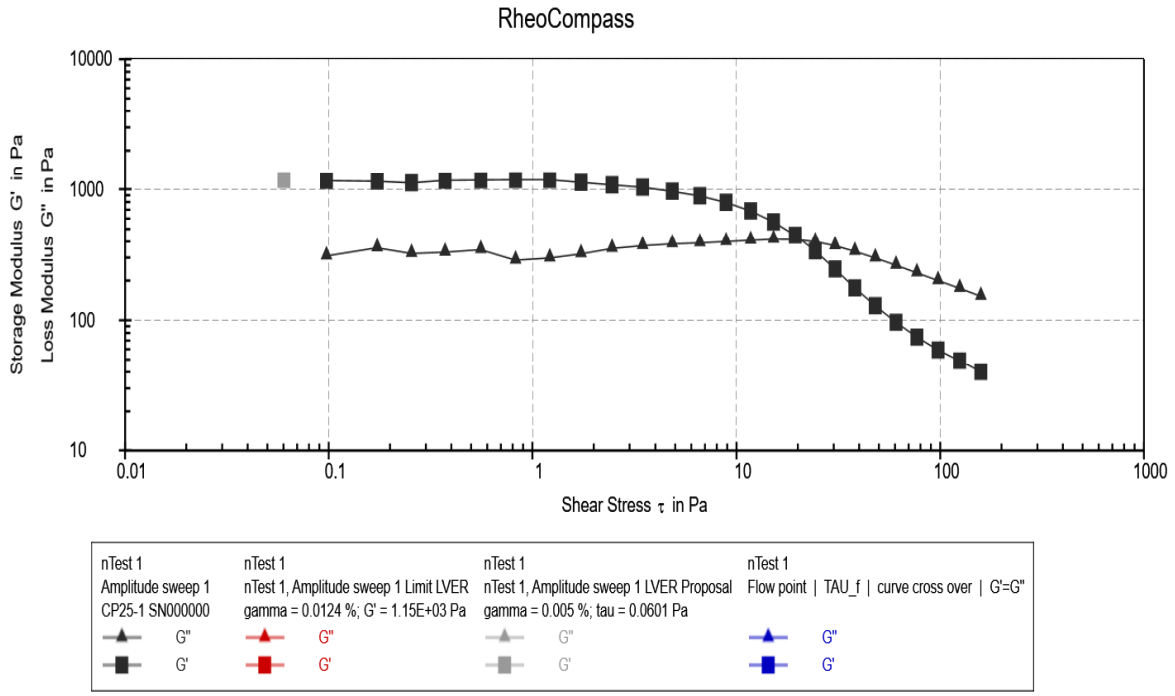

Figure 5.15 B. Amplitude sweep test of Apremilast loaded LCNPs gel

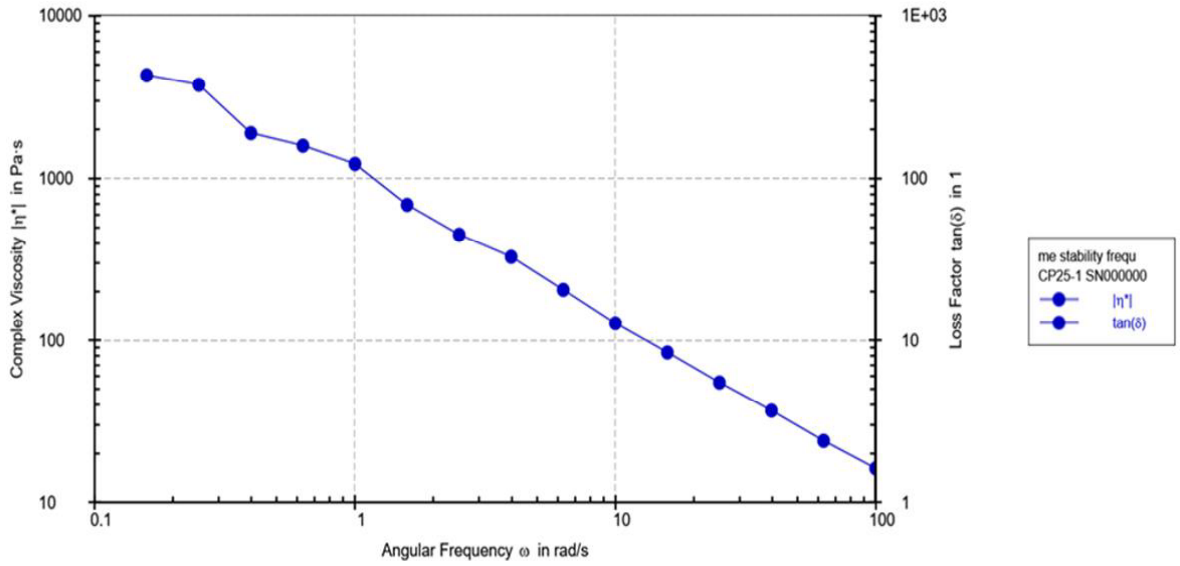

Figure 5.15 C. Frequency sweep test of Apremilast loaded LCNPs gel formulation (Complex viscosity).

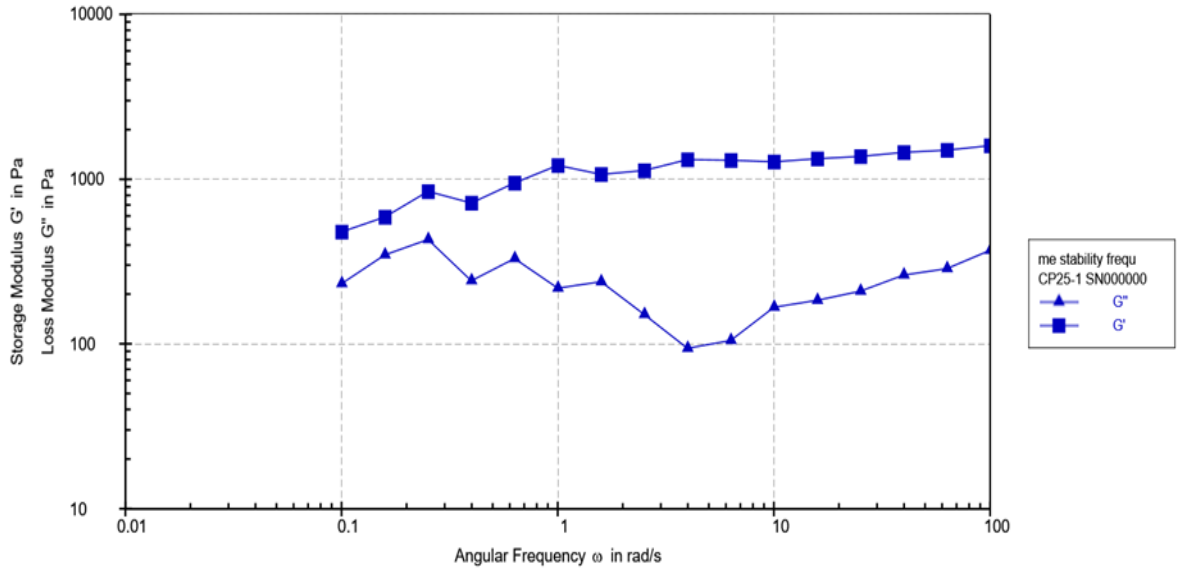

Figure 5.15 D. Frequency sweep test of Apremilast loaded LCNPs gel (loss modulus and storage modulus).

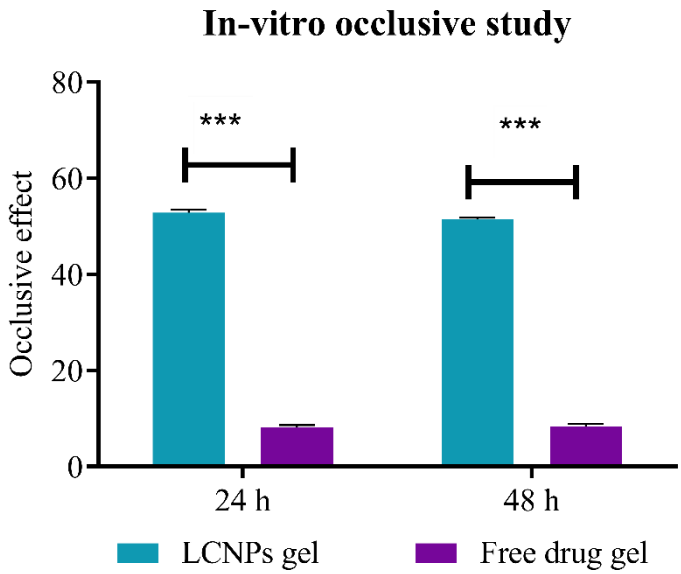

Figure 5.16. The in-vitro occlusive study of the Apremilast loaded LCNPs gel (Mean ± SD, n = 3) (***p<0.0001).

5.3.9.2. Ex-vivo skin permeation and skin retention study

The ex-vivo skin permeation studies performed through goat ear skin revealed improved permeation with LCNPs gel formulation compared to free drug-loaded gel. The transdermal flux of the Apremilast loaded LCNPs gel was 0.2747 (µg/h/cm^2), and the free drug-loaded gel

was 0.1706 (µg/h/cm^2). The Apremilast loaded LCNPs gel flux was 1.6 fold higher compared to free drug-loaded gel indicating high permeation of Apremilast loaded LCNPs gel. The permeability coefficient of LCNPs formulation and the free drug-loaded gel was found to be 0.916 $\times 10^{-2}$ and 0.569 $\times 10^{-2}$, respectively. The skin retention studies showed that the amount of drug retained with LCNPs formulation was found to be 23.057 ± 2.934 µg/cm^2 and 51.652 ± 5.023 µg/cm^2 in stratum corneum and viable part of skin, respectively. The ex-vivo skin permeation and skin retention data are illustrated in the **Figure 5.17 A and 5.17 B.**

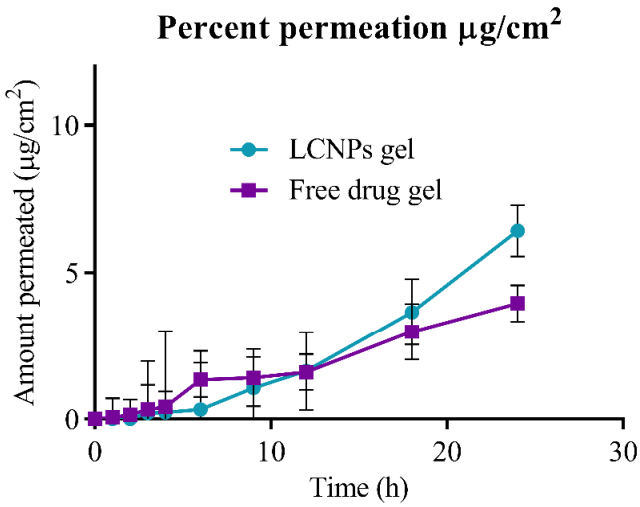

Figure 5.17 A. Ex-vivo skin permeation profiles of Apremilast loaded LCNPs gel compared with free drug-loaded gel (Mean ± SD, n=3)

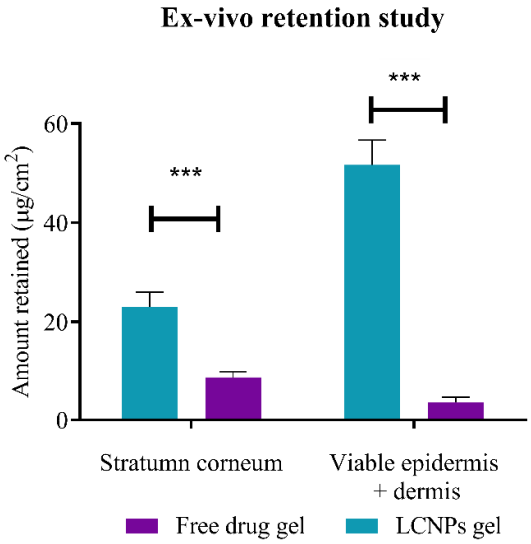

Figure 5.17 B. Skin retention study of Apremilast loaded LCNPs gel compared with free drug-loaded gel (Mean ± SD, n=3) (***p<0.0001).

The amount of drug retained with free drug-loaded gel was found to be 8.845 ± 1.140 μg/cm^2 and 3.548 ± 1.066 μg/cm^2 in stratum corneum and viable part of the skin, respectively. The amount of drug retention with LCNPs formulation in stratum corneum and viable part of skin was found to be 2.61 and 14.59 fold higher, respectively. The ex-vivo studies revealed low skin permeation and high skin retention studies. The nanosize of the formulation and amount of lipid favors the formation of the occlusive film. The occlusive film formation reduces the TEWL, which further increases the hydration of the skin. The hydration of the skin increases gaps in corneocytes and skin permeation. The studies suggest that the permeation of liquid crystals on topical application follows the intercellular path. This was the expected reason for high retention in the viable part of the skin [3,15]. Liquid crystal-based formulation exhibits high hydration and easy distribution compared to the emulsion due to the similarity in the structures of LC and stratum corneum. The cubic phase system exhibits strong bio-adhesive property and forms a biological membrane like structure over the skin on topical application. The cubic phase is expected to interact with the stratum corneum forming a cubosomal lipid-stratum corneum lipid mixture and form cubosome depot which releases the drug in a controlled manner [16]. The amphiphilic nature of lipid and the presence of surfactant in the liquid crystals favour the interaction with stratum corneum and increase the drug permeability [17]. The drugs encapsulated in LCNP interact with the skin tissue and localize in the stratum corneum resulting in the controlled release of the drug. This attributes to the minimal systemic absorption thus reducing the adverse effects. The presence of water in liquid crystals act as reservoir and provides hydration to the tissue [18].

5.3.9.3. Ex-vivo skin distribution studies

The skin distribution of the selected LCNPs formulation was determined qualitatively using Coumarin-6 dye. The Coumarin-6 loaded LCNPs formulation was prepared by replacing Apremilast with Coumarin-6. The study performed for 8 h and 16 h demonstrated the improved

permeation of Coumarin-6 loaded LCNPs compared to free Coumarin-6. The skin distribution study results are represented in **Figure 5.18**. The improved permeation with LCNPs formulation was expected due to nanosize and occlusive effect [19].

5.3.9.4. Dermatocokinetic estimation

The $C_{maxSkin}$ of the Apremilast LCNPs loaded gel was found to be 189.744 ± 2.220 µg/cm^2 and 66.824 ± 8.528 µg/cm^2 in epidermis and dermis, respectively. The $C_{maxSkin}$ of the free drug-loaded gel was found to be 41.768 ± 2.518 µg/cm^2 and 13.047 ± 3.107 µg/cm^2 in epidermis and dermis, respectively. The T_{max} of LCNPs formulation was found to be 6 h in the epidermis and dermis, whereas the T_{max} for the free drug-loaded gel was found to be 6 h in the epidermis and 8 h in the dermis. The $AUC_{0–24}$ of the Apremilast LCNPs loaded gel was found to be 8.84 fold higher in epidermis (2872.747 ± 93.701 µg/cm^2.h) compared to free drug-loaded gel (324.840 ± 8.828 µg/cm^2.h). In dermis the Apremilast LCNPs loaded gel (550.750 ± 155.88 µg/cm^2.h) exhibited 2.69 fold higher compared to free drug-loaded gel (204.343 ± 8.482 µg/cm^2.h). The dermatokinetic parameters of Apremilast LCNPs loaded gel and free drug-loaded gel are presented in **Table 5.9,** and the dermatokinetic profile is illustrated in **Figure 5.19 A and Figure 5.19 B**. The LCNPs formulation exhibited high drug concentration in skin layers. The T_{max} of LCNPs formulation was faster compared to the free drug, which indicates improved permeation in LCNPs formulation. The results suggest that the drug diffuses into deeper layers of the skin, and it was retained for a longer duration of time [20]. The interaction between the skin lipids and the polar head group and non-polar chain of LCNPs lipid helps in embedding of nanoparticles in skin.

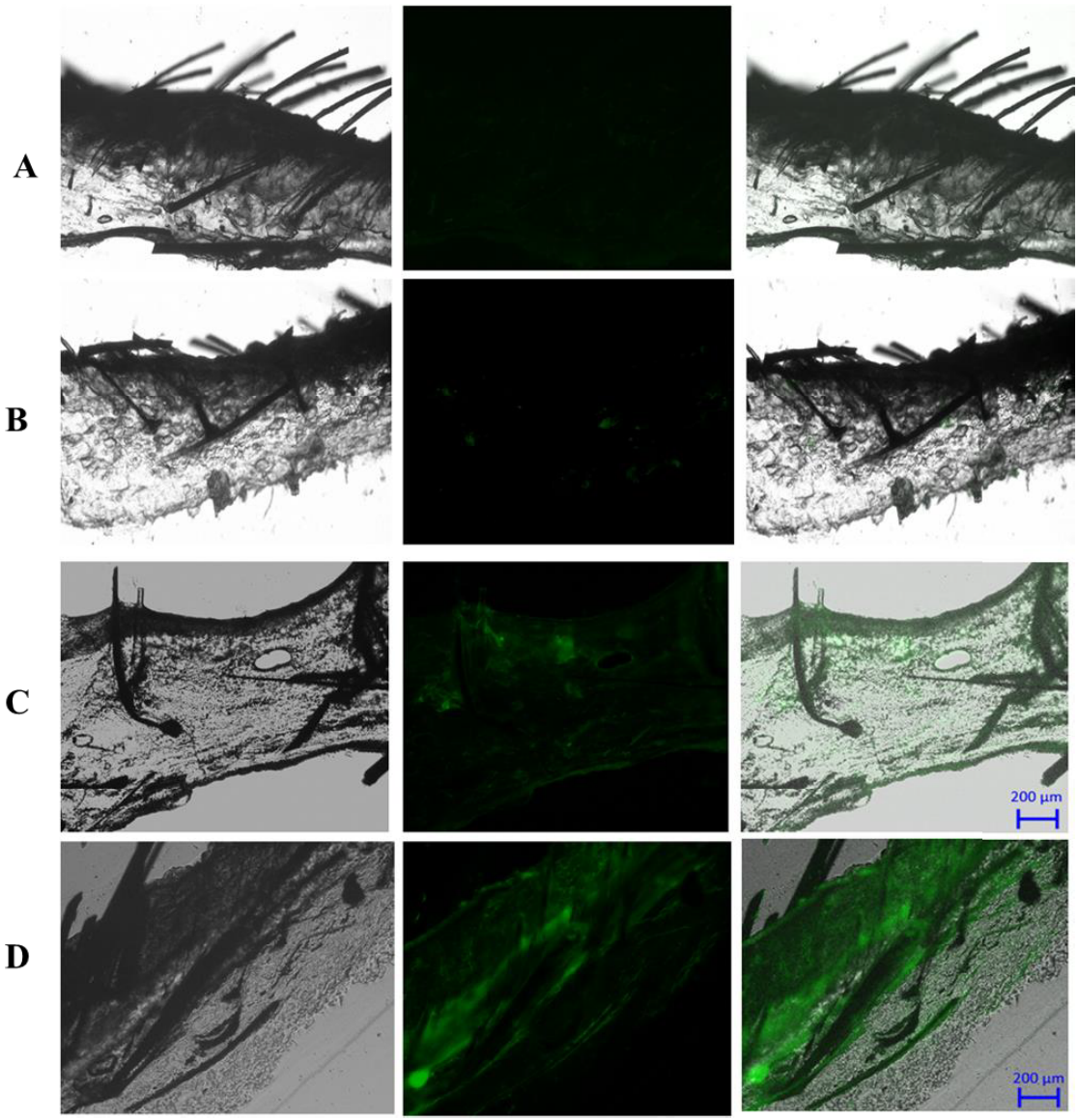

Figure 5.18. In-vitro skin retention studies using Coumarin-6 loaded LCNPs dispersion and free Coumarin-6 dispersion. **(A)** Skin treated with free Coumarin-6 for 8 h; **(B)** Skin treated with free Coumarin-6 for 16 h; **(C)** Skin treated with Coumarin-6 loaded LCNPs dispersion for 8 h; **(D)** kin treated with Coumarin-6 loaded LCNPs dispersion for 16 h.

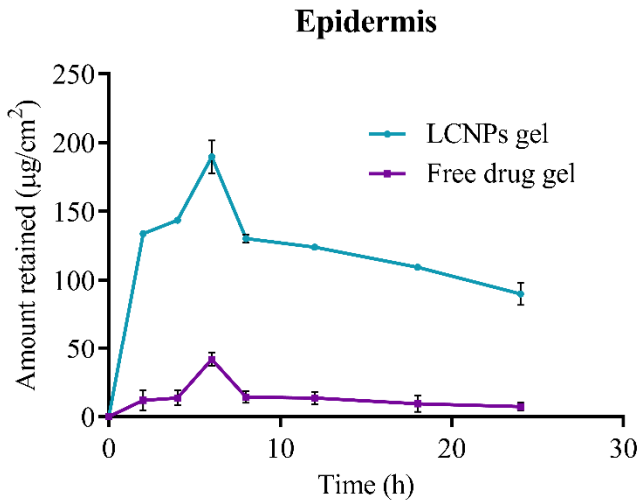

Figure 5.19 A. Dermatokinetic profile of Apremilast loaded LCNPs gel compared with free drug loaded gel in the epidermis (Mean ± SD, n=4) (***p<0.0001)

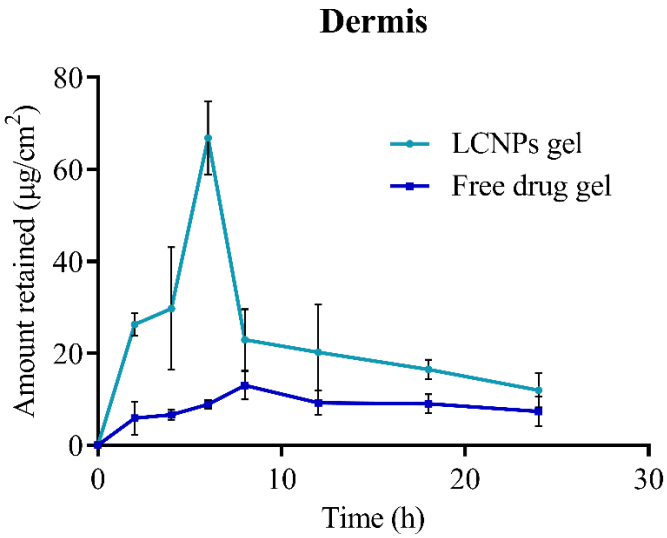

Figure 5.19 B. Dermatokinetic profile of Apremilast loaded LCNPs gel compared with free drug-loaded gel in the dermis (Mean ± SD, n=4) (***p<0.0001).

Table 5.9. Summary of dermatokinetic parameters of Apremilast LCNPs loaded gel and free drug-loaded gel (n=4).

Parameter	Apremilast LCNPs loaded gel		Free drug-loaded gel	
	Epidermis	Dermis	Epidermis	Dermis
$AUC_{0–24}$ (µg/cm².h)	2872.747 ± 93.701	550.750 ± 155.88	324.840 ± 8.828	204.343 ± 8.482
$AUC_{0\text{-}inf}$ (µg/cm².h)	6257.886 ± 1419.22	846.263 ± 321.01	465.389 ± 7.100	442.657 ± 62.786
$C_{maxSkin}$ (µg/cm²)	187.744 ± 2.22	66.824 ± 8.53	41.768 ± 2.518	13.047 ± 3.107
T_{max} (h)	6.00	6.00	6.00	8.00
Ke (h^{-1})	0.026 ± 0.014	0.040 ± 0.024	0.052 ± 0.001	0.030 ± 0.010

5.3.10. In-vivo skin retention and irritation studies

The amount of drug retained (µg/cm²) in skin layers of swiss albino mice treated with Apremilast loaded LCNPs gel and free drug-loaded gel after 12 h and 24 h are illustrated in **Figure 5.20.** The amount of drug retained in the skin was higher in LCNPs loaded gel formulation (4.44 fold in 12 h, 2.59 fold higher in 24 h) than free drug-loaded gel. The amount of drug retained in the stratum corneum and viable part of the skin treated with Apremilast loaded LCNPs gel and free drug-loaded gel are represented in **Table 5.10.**

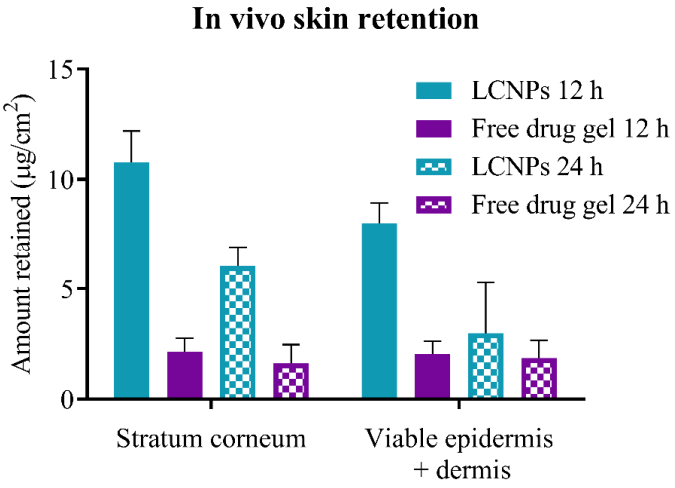

Figure 5.20. Skin retention of Apremilast in swiss albino mice treated with LCNPs loaded gel, and free drug-loaded gel for 12 h and 24 h.

Table 5.10. Amount of Apremilast retained in the skin layers

Formulation		Skin layers	
		Stratum Corneum (µg/cm^2)	**Viable epidermis + dermis (µg/cm^2)**
LCNPs gel	**12 h**	10.77 ± 1.42	8.00 ± 0.94
	24 h	6.03 ± 0.90	2.98 ± 2.30
Free drug-loaded gel	**12 h**	2.16 ± 0.60	2.06 ± 0.56
	24 h	1.62 ± 0.85	1.85 ± 0.82

The data revealed a high drug concentration in 12 h compared to 24 h in animals treated with Apremilast-loaded LCNPs gel. As the data obtained in the dermatokinetic study, T_{max} achieved was 8 h, indicating a higher drug concentration in 12h compared to 24 h. The amount of drug retained was higher in Apremilast loaded LCNPs gel compared to free drug preparation. The amount of drug in the stratum corneum after 12 h was similar in three formulations. However, the amount of drug in deeper layers after 12 h was higher in LCNPs (LCNPs > NLCs > SLNs). The obtained results indicate that the LCNPs formulation exhibit deeper permeation due to the interaction, which might result in the transition of the ordered hexagonal or orthorhombic lipids to the disordered fluid lamellar liquid crystalline phase. This subsequently affects the permeation rate through paracellular spaces of the skin, for not only the entrapped drug but also the free drug through the skin. In general, disordered liquid crystalline phases show better permeability overordered lipid phases of the skin. The drug retained in skin layers up to 24 h indicates that the developed formulation can exhibit prolonged retention in skin layers [21,22].

The skin irritation studies showed no signs of irritation (inflammation and erythema) on the skin in 12 h and 24 h after applying the gel, as illustrated in **Figure 5.21**. The skin histology study showed that there were no signs of inflammation or changes in the skin. The H&E staining histology data is represented in **Figure 5.22**. The data showed that the skin structure was intact and normal [23,24]. The results indicate that the developed LCNPs formulation is

safe for topical delivery of Apremilast. The developed lipid formulations can improve permeation and skin retention for a prolonged time duration.

5.3.11. Storage stability of Apremilast loaded LCNPs gel

The Apremilast loaded LCNPs gel depicted nanocarriers' integrity using Malvern zeta sizer without any aggregation. The assay results depicted no substantial change (< 2%) as represented in **Table 5.11**, indicating the stability of Apremilast loaded LCNPs gel [25,26].

Table 5.11. Stability data of Apremilast loaded LCNPs gel (n=3).

Stability data of LCNPs dispersion loaded gel at 4˚C				
Parameter	**0 Month**	**1 Month**	**2 Month**	**3 Month**
Assay of gel (%)	100.00 ± 0.560	99.95 ± 0.735	99.92 ± 0.305	99.87 ± 0.543
Size (nm)	181.50 ± 4.872	183.43 ± 3.360	185.60 ± 2.793	189.10 ± 3.857
PDI	0.261 ± 0.004	0.267 ± 0.020	0.289 ± 0.008	0.271 ± 0.080
Stability data of LCNPs dispersion loaded gel at 25˚C				
Assay of gel (%)	100.00 ± 0.560	99.91 ± 0.682	99.89 ± 0.251	99.74± 0.587
Size (nm)	181.50 ± 4.872	184.40 ± 3.616	189.60 ± 2.469	192.59 ± 4.440
PDI	0.261 ± 0.004	0.233 ± 0.012	0.252 ± 0.123	0.254 ± 0.017

Formulation	Before application of gel	After application of gel
LCNPs loaded gel	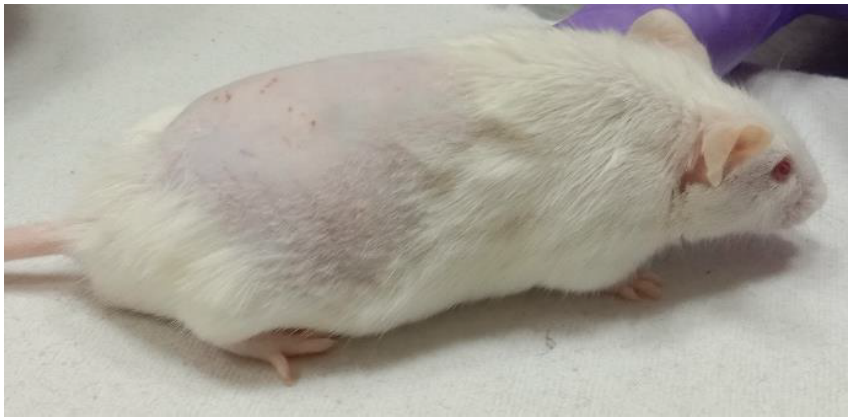	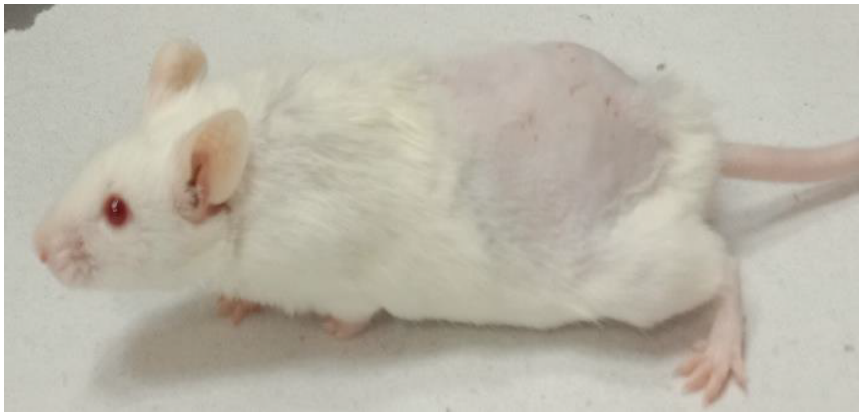
Free drug-loaded gel	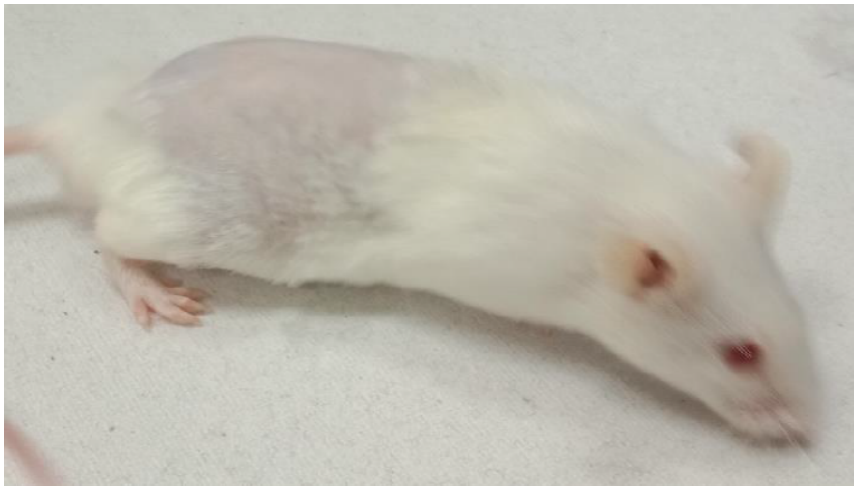	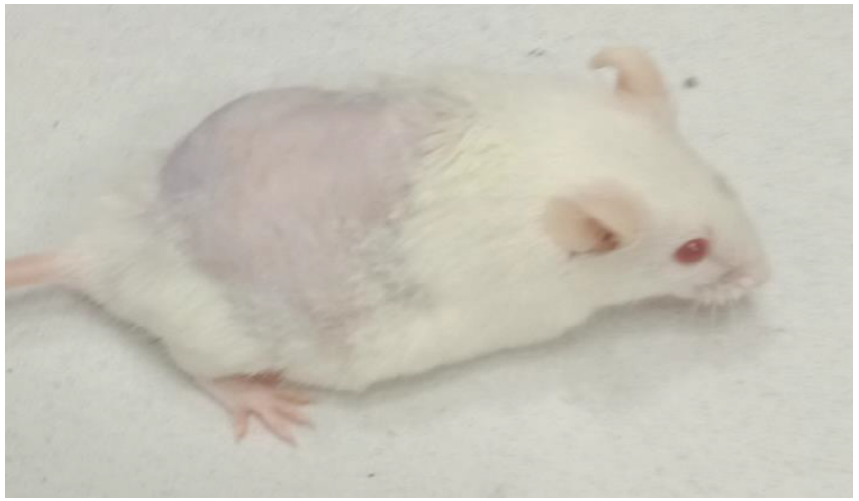

Figure 5.21. The animal images for signs of irritation (inflammation and erythema) after and before application.

Formulation	12 h	24 h
LCNPs loaded gel	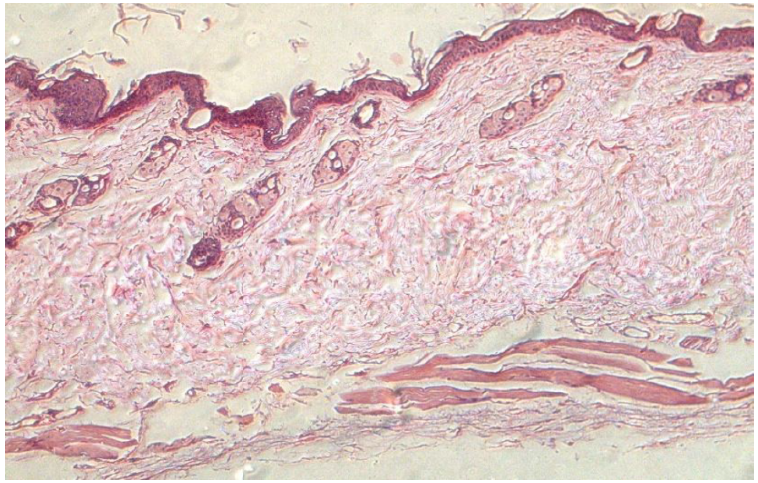	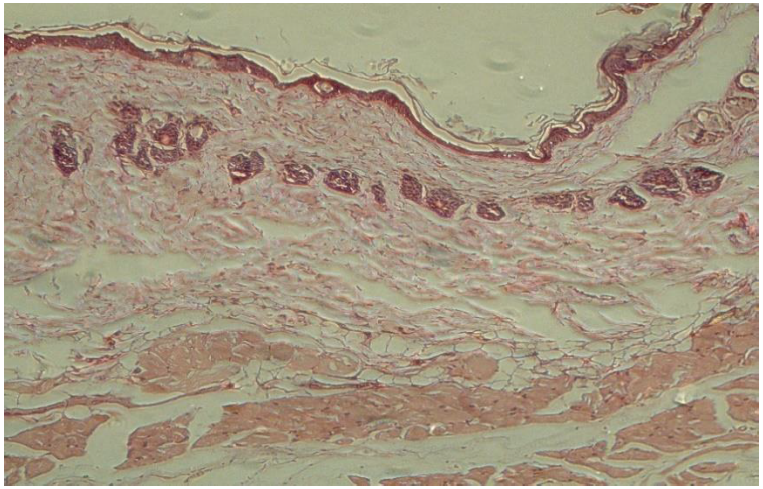
Free drug-loaded gel	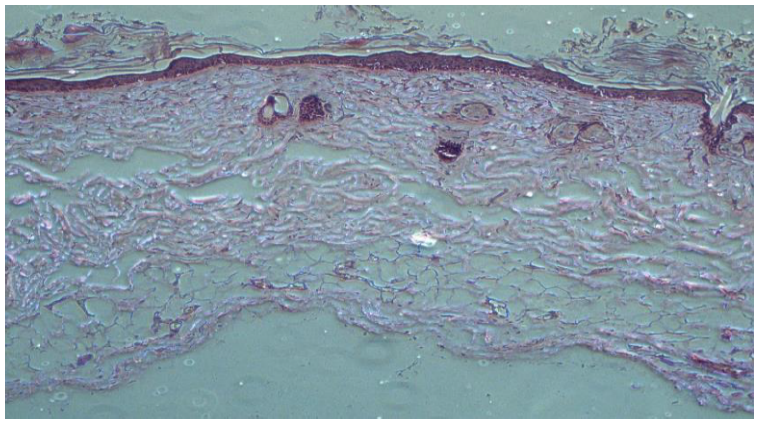	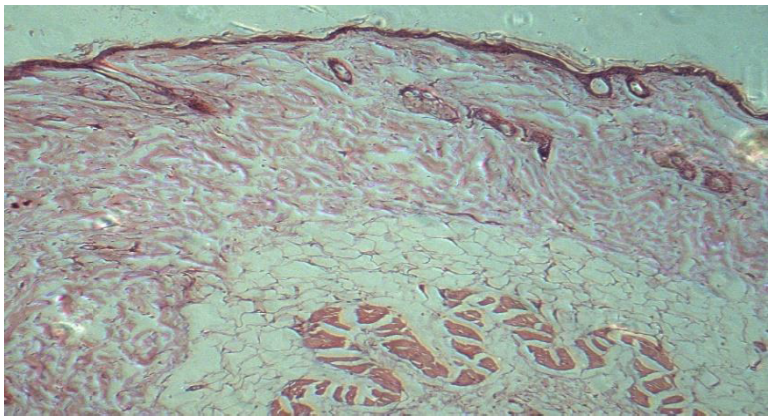

Control (without application of formulation)

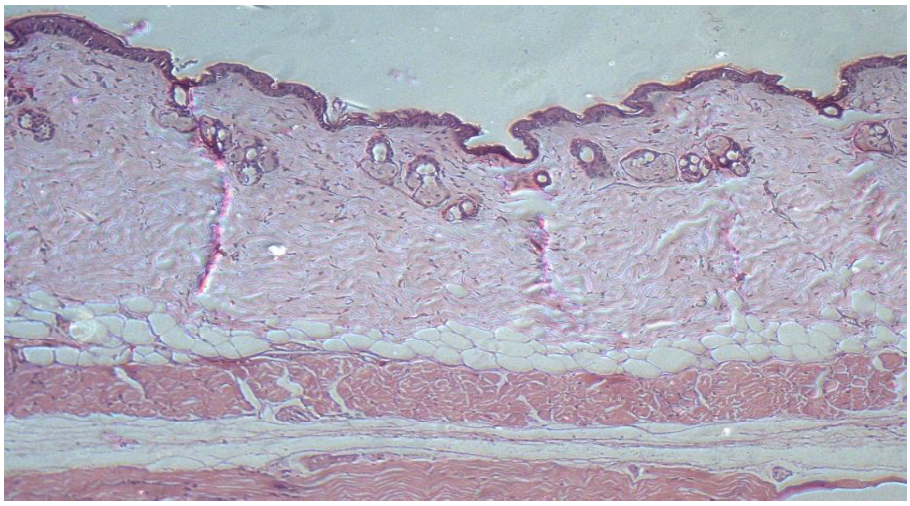

Figure 5.22. The H&E staining histology data after 12 h and 24 h of application

5.4. Conclusion

Apremilast loaded LCNPs formulation was developed by emulsification using a high shear homogenizer. The formulation was optimized using the Box-Behnken design. The optimized formulation showed smaller particle size and PDI, which augments skin permeation. The in-vitro drug release showed formulation exhibited prolonged release with enhanced skin retention. The formulation was found to be non-toxic in cell viability studies, and no irritation/erythema was observed in the in-vivo skin irritation study. The prepared LCNP formulation results portrayed improved permeation and retention in swiss albino mice. The results confirm that the selected LCNPs formulation can be utilized for topical delivery of Apremilast to treat psoriasis.

References

[1] V.K. Rapalli, T. Waghule, N. Hans, A. Mahmood, S. Gorantla, S.K. Dubey, G. Singhvi, Insights of lyotropic liquid crystals in topical drug delivery for targeting various skin disorders, J. Mol. Liq. 315 (2020) 113771. https://doi.org/10.1016/j.molliq.2020.113771.

[2] A. Mahmood, V.K. Rapalli, T. Waghule, S. Gorantla, G. Singhvi, Luliconazole loaded lyotropic liquid crystalline nanoparticles for topical delivery: QbD driven optimization, in-vitro characterization and dermatokinetic assessment, Chem. Phys. Lipids. 234 (2021) 105028. https://doi.org/10.1016/j.chemphyslip.2020.105028.

[3] T. Waghule, S. Patil, V.K. Rapalli, V. Girdhar, S. Gorantla, S. Kumar Dubey, R.N. Saha, G. Singhvi, Improved skin-permeated diclofenac-loaded lyotropic liquid crystal nanoparticles: QbD-driven industrial feasible process and assessment of skin deposition, Liq. Cryst. 0 (2020) 1–19. https://doi.org/10.1080/02678292.2020.1836276.

[4] E.S. Behbahani, M. Ghaedi, M. Abbaspour, K. Rostamizadeh, Optimization and characterization of ultrasound assisted preparation of curcumin-loaded solid lipid nanoparticles: Application of central composite design, thermal analysis and X-ray diffraction techniques, Ultrason. Sonochem. 38 (2017) 271–280. https://doi.org/10.1016/j.ultsonch.2017.03.013.

[5] G. Schett, V.S. Sloan, R.M. Stevens, P. Schafer, Apremilast: A novel PDE4 inhibitor in the treatment of autoimmune and inflammatory diseases, Ther. Adv. Musculoskelet. Dis. 2 (2010) 271–278. https://doi.org/10.1177/1759720X10381432.

[6] H. Yuan, J. Miao, Y.Z. Du, J. You, F.Q. Hu, S. Zeng, Cellular uptake of solid lipid nanoparticles and cytotoxicity of encapsulated paclitaxel in A549 cancer cells, Int. J. Pharm. 348 (2008) 137–145. https://doi.org/10.1016/j.ijpharm.2007.07.012.

[7] S.R. Varma, T.O. Sivaprakasam, A. Mishra, S. Prabhu, M. Rafiq, P. Rangesh, Imiquimod-induced psoriasis-like inflammation in differentiated Human keratinocytes: Its evaluation using curcumin, Eur. J. Pharmacol. 813 (2017) 33–41. https://doi.org/10.1016/j.ejphar.2017.07.040.

[8] J. Sun, Y. Zhao, J. Hu, Curcumin Inhibits Imiquimod-Induced Psoriasis-Like Inflammation by Inhibiting IL-1beta and IL-6 Production in Mice, PLoS One. 8 (2013)

e67078. https://doi.org/10.1371/journal.pone.0067078.

[9] N. Shraibom, A. Madaan, V. Joshi, R. Verma, A. Chaudhary, G. Mishra, A. Awasthi, A.T. Singh, M. Jaggi, Evaluation of in vitro Anti-psoriatic Activity of a Novel Polyherbal Formulation by Multiparametric Analysis, Antiinflamm. Antiallergy. Agents Med. Chem. 16 (2017). https://doi.org/10.2174/1871523016666170720160037.

[10] P. R. Varges, C. M. Costa, B. S. Fonseca, M. F. Naccache, P. De Souza Mendes, Rheological Characterization of Carbopol® Dispersions in Water and in Water/Glycerol Solutions, Fluids. 4 (2019) 3. https://doi.org/10.3390/fluids4010003.

[11] C. Gazga-Urioste, E. Rivera-Becerril, G. Pérez-Hernández, N. Angélica Noguez-Méndez, A. Faustino-Vega, C. Tomás Quirino-Barreda, Physicochemical characterization and thermal behavior of hexosomes containing ketoconazole as potential topical antifungal delivery system, Drug Dev. Ind. Pharm. 45 (2019) 168–176. https://doi.org/10.1080/03639045.2018.1526188.

[12] L.Q. Ying, M. Misran, Rheological and physicochemical characterization of alpha-tocopherol loaded lipid nanoparticles in thermoresponsive gel for topical application, Malaysian J. Fundam. Appl. Sci. 13 (2017) 248–252. https://doi.org/10.11113/mjfas.v13n3.596.

[13] J. Simta, I. Kavita, B. Milind, Novel Long Retentive Posaconazole Ophthalmic Suspension, 6 (2020) 1–10. https://doi.org/10.11648/j.pst.20200401.11.

[14] V. Kakkar, I.P. Kaur, A.P. Kaur, K. Saini, K.K. Singh, Topical delivery of tetrahydrocurcumin lipid nanoparticles effectively inhibits skin inflammation: in vitro and in vivo study, Drug Dev. Ind. Pharm. 44 (2018) 1701–1712. https://doi.org/10.1080/03639045.2018.1492607.

[15] G. Singhvi, S. Hejmady, V.K. Rapalli, S.K. Dubey, S. Dubey, Nanocarriers for topical delivery in psoriasis, in: R. Shegokar (Ed.), Deliv. Drugs, Elsevier Inc., Germany, 2020: pp. 75–96. https://doi.org/10.1016/b978-0-12-817776-1.00004-3.

[16] N.R. Rarokar, S.D. Saoji, N.A. Raut, J.B. Taksande, P.B. Khedekar, V.S. Dave, Nanostructured Cubosomes in a Thermoresponsive Depot System: An Alternative Approach for the Controlled Delivery of Docetaxel, AAPS PharmSciTech. 17 (2016) 436–445. https://doi.org/10.1208/s12249-015-0369-y.

[17] M.H. Oyafuso, F.C. Carvalho, L.A. Chiavacci, M.P.D. Gremião, M. Chorilli, Design and characterization of silicone and surfactant based systems for topical drug delivery, J. Nanosci. Nanotechnol. 15 (2015) 817–826. https://doi.org/10.1166/jnn.2015.9181.

[18] R. Rajabalaya, M.N. Musa, N. Kifli, S.R. David, Drug Design, Development and Therapy Dovepress Oral and transdermal drug delivery systems: role of lipid-based lyotropic liquid crystals, (2017) 11–393. https://doi.org/10.2147/DDDT.S103505.

[19] S. Jain, R. Addan, V. Kushwah, H. Harde, R.R. Mahajan, Comparative assessment of efficacy and safety potential of multifarious lipid based Tacrolimus loaded nanoformulations, Int. J. Pharm. 562 (2019) 96–104. https://doi.org/10.1016/j.ijpharm.2019.03.042.

[20] M.S. Freag, A.S. Torky, M.M. Nasra, D.A. Abdelmonsif, O.Y. Abdallah, Liquid crystalline nanoreservoir releasing a highly skin-penetrating berberine oleate complex for psoriasis management, Nanomedicine. 14 (2019) 931–954. https://doi.org/10.2217/nnm-2018-0345.

[21] R. Sonawane, H. Harde, M. Katariya, S. Agrawal, S. Jain, Solid lipid nanoparticles-loaded topical gel containing combination drugs: An approach to offset psoriasis, Expert Opin. Drug Deliv. 11 (2014) 1833–1847. https://doi.org/10.1517/17425247.2014.938634.

[22] P.M. Al-Maghrabi, E.S. Khafagy, M.M. Ghorab, S. Gad, Influence of formulation variables on miconazole nitrate–loaded lipid based nanocarrier for topical delivery, Colloids Surfaces B Biointerfaces. 193 (2020) 111046. https://doi.org/10.1016/j.colsurfb.2020.111046.

[23] J. Sun, W. Dou, Y. Zhao, J. Hu, A comparison of the effects of topical treatment of calcipotriol, camptothecin, clobetasol and tazarotene on an imiquimod-induced psoriasis-like mouse model, Immunopharmacol. Immunotoxicol. 36 (2014) 17–24. https://doi.org/10.3109/08923973.2013.862542.

[24] A. Dadwal, N. Mishra, R.K. Rawal, R.K. Narang, Development and characterisation of clobetasol propionate loaded Squarticles as a lipid nanocarrier for treatment of plaque psoriasis, J. Microencapsul. (2020) 1–14. https://doi.org/10.1080/02652048.2020.1756970.

[25] V.A. Guilherme, L.N.M. Ribeiro, A.C.S. Alcântara, S.R. Castro, G.H. Rodrigues da Silva, C.G. da Silva, M.C. Breitkreitz, J. Clemente-Napimoga, C.G. Macedo, H.B. Abdalla, R. Bonfante, C.M.S. Cereda, E. de Paula, Improved efficacy of naproxen-loaded NLC for temporomandibular joint administration, Sci. Rep. 9 (2019) 1–11. https://doi.org/10.1038/s41598-019-47486-w.

[26] S. Khurana, P.M.S. Bedi, N.K. Jain, Preparation and evaluation of solid lipid nanoparticles based nanogel for dermal delivery of meloxicam, Chem. Phys. Lipids. 175–176 (2013) 65–72. https://doi.org/10.1016/j.chemphyslip.2013.07.010.